The Role of the Receptor for Advanced Glycation End Products (RAGE) in idiopathic Pulmonary Fibrosis

Inaugural Dissertation
Zur Erlangung des Doktorgrades der
Naturwissenschaften
-Dr. rer. nat.-
vorgelegt von

Markus Alexander Queisser
aus Berlin, Deutschland

angefertigt am Institut für Biochemie
Fachbereich Medizin und dem Fachbereich für Biologie
und Chemie
Justus-Liebig-Universität Giessen

From the Department of Medicine
Institute of Biochemistry
Director: Prof. Dr. Klaus T. Preissner
at the Justus Liebig University Giessen

First Supervisor and Committee Member **Prof. Dr. A. Pingoud**

Second Supervisor and Committee Member **Prof. Dr. K.T. Preissner**

Committee members: Prof. Dr. W. Clauss and Prof. Dr. R. Dammann

Date of Doctoral Defense ·····15.05.2009

“Forschung ist nie zu Ende, sie lebt von der Kritik und der intelligenten Skepsis, die nicht die Arroganz des Ignoranten ist.“

Prof. Dr. Lothar Jaenicke

List of figures

Figures Introduction

Figures Results

List of abbreviations

Aβ = Amyloid-beta
ADAM = A Disintegrin And Metalloproteinase protein
AEC = alveolar epithelial cells
AGE = Advanced Glycation End Products
ALI = Acute lung injury
ARDS = Acute respiratory distress syndrome
AT = Alveolar type
ATP = Adenosin triphosphate
BAL = Bronchoalveolar lavage fluid
BCA = Bicinchoninic acid
Bcl-2 = B-cell lymphoma 2
CD = Cluster of differentiation
CML = Carboxymethyl lysine
CMPC = Circulating mesenchymal progenitor cells
Col = Collagen
CT = Cycle of threshold
CXCR = Chemokine-CXC-motif Receptor
DMEM = Dulbecco's modified Eagle medium
DNA = Deoxyribonucleic acid
dNTP = Desoxy nucleotide triphosphate
DTT = DL-Dithiothreitol
EC = Endothelial Cell
ECL = Enhanced Chemiluminescence
ECM = Extracellular matrix
EDTA = Eythelene diamino tetra acetic acid
Egr-1 = Early growth factor-1
EF = Elongation factor
EMT = Epithelial-mesenchymal transition
EN-RAGE = Extracellular newly identified RAGE binding protein (S100A12)

ERK = Extracellular signal-regulated kinase
esRAGE = Endogenous soluble RAGE
FBS = Fetal bovine serum
FGF-2 = Fibroblast growth factor 2
FITC = Fluorescein isothiocyanate
FSP-1 = Fibroblast specific protein
GTPase = GTP hydrolase
GTP = Guanosine triphosphate
HBSS = Hank's Buffered Salt Solution
HEPES = 4-(2-hydroxyethyl)-1-piperazineethanesulfonic acid
HGF = Hepatocyte growth factor
Hmbs = Hydroxymethylbilane synthase
HMGB1 = High mobility group binding-protein B1
HRP = Horse-radish peroxidase
ICAM-1 = Inter-Cellular Adhesion Molecule 1
IgG = Immune globuline
IL-1β = Interleukin-1β
IL-6 = Interleukin-6
ILD = Interstitial lung diseases
IFN-α = Interferon-α
IPF = Idiopathic Pulmonary Fibrosis
JNK = C-Jun-N-terminal kinase
KGF = Keratinocyte growth factor
MAPK = Mitogen-activated protein kinase
MCP-1 = Monocyte chemotactic protein-1
MMP = Matrix Metalloprotease
mRNA = messenger RNA
miRNA = micro RNA
NADPH = Nicotinamide adenine dinucleotide phosphate
NF-κB = Nuclear factor -κB
pDC = Plasmacytoid dendritic cells
PAI-1 = Plasminogen-activator inhibitor 1
PCR = Polymerase chain reaction

PBS = Phosphate buffered saline
PDGF = Platelet derived growth factor
PI3K = Phosphoinositide kinase 3
PMVEC = Pulmonary microvascular endothelial cells
PRP = Pattern recognition receptor
PDVF = Polyvinylidene difluoride
RAGE = Receptor for Advanced Glycation End Products
RBC = Red blood cells
RNA = Ribonucleic acid
RNP = Ribonucleoprotein
SDS = Dodecyl sodium salt
siRNA = Small interfering RNA
SMA = Smooth muscle actin
SP-C = Surfactant protein C
sRAGE = Soluble RAGE
ROS = Reactive oxygen species
RT = Reverse Transcriptase
TBS = Tris buffered saline
TBST = Tris buffered saline tween
TEMED = N,N,N',N'-Tetramethylethylenediamine
TERT = Telomerase reverse transcriptase
TF = Tissue factor
TIMP = Tissue inhibitors of MMP
TGF-β = Tumor growth factor-β
TLR = Toll-like receptor
TNF-α = Tumor-necrosis factor-α
TR = Telomerase RNA
TRIS = Tris(hydroxymethyl)aminomethane
UIP = Usual interstitial pneumonia
UTR = Untranslated region
VCAM-1 = Vascular cellular adhesion molecule 1
ZO-1 = Zonula occludens-1

Summary

The Receptor for Advanced Glycation End Products (RAGE) is a transmembrane receptor of the immunoglobulin superfamily. While vascular RAGE expression is associated with kidney and liver fibrosis, under physiological conditions high expression level of RAGE is found in the lung. In this work, RAGE expression in idiopathic pulmonary fibrosis (IPF) was assessed, and the relation of the receptor to functional changes of epithelial cells and pulmonary fibroblasts in the pathogenesis of the disease was investigated. Significant downregulation of RAGE was observed in lung homogenate and alveolar epithelial cells (AEC) type II from IPF patients as well as in bleomycin-treated mice, demonstrated by RT-PCR, western blotting and immunohistochemistry. RAGE downregulation was provoked by stimulation of primary human lung fibroblasts and A549 epithelial cells with the pro-inflammatory cytokines, transforming growth factor-β1 or tumor necrosis factor-α *in vitro*. Blockade of RAGE resulted in impaired cell adhesion, and siRNA induced knock down of RAGE increased cell proliferation and migration of A549 cells and human primary fibroblasts *in vitro*. These results indicate that RAGE serves a protective role in the lung and that loss of the receptor is related with functional changes of pulmonary cell types with the consequences of fibrotic disease. The study provides evidence that the expression and regulation of RAGE in the pulmonary system differs from that in the vascular system. Here, a possible functional mechanism of RAGE in pulmonary fibrosis is described for the first time.

Zusammenfassung

Der Rezeptor für “Advanced glycation end products” (RAGE) ist ein Transmembranrezeptor aus der Superfamilie der Immunglobuline. Die vaskuläre RAGE Expression ist mit Nieren- und Leberfibrose assoziert, während eine hohe Expression von RAGE in der Lunge unter normalen physiologischen Bedingungen gefunden wurde. In dieser Studie wurde die Expression von RAGE in Patienten der idiopathischen Lungenfibrose (IPF) gemessen, und die Beziehung zwischen RAGE und die funktionellen Änderungen von Epithelzellen und pulmonalen Fibroblasten wurde untersucht. Signifikante Absenkung der Expression von RAGE wurde in Lungenhomogenaten und isolierten alveolaren Epithelzellen type II von IPF Patienten sowie auch in Bleomycin-behandelten Mäusen, nachgewiesen mittels RT-PCR, Western-blot und Immohistochemie. *In vitro* wurde die Repression von RAGE durch die pro-inflammatorischen Zytokine TGF-β und TNF-α in primären Fibroblasten und A549 Epithelzellen erreicht. Desweiteren führte die Blockade von RAGE mittels anti-RAGE Antikörpern zu reduzierter Zelladhäsion. siRNA-induzierte Inhibierung der Expression von RAGE in A549 und Fibroblasten führte zur vermehrten Zellproliferation und -Migration *in vitro*.

Diese Ergebnisse deuten auf eine Schutzfunktion der RAGE Expression in der Lunge hin, hingegen trägt der Verlust an RAGE zu zellulären Änderungen und fibrotischen Erkrankungen bei. Diese Studie deckt molekulare Zusammenhänge auf, die zur Erklärung der Unterschiede in der Expression und Regulation von RAGE zwischen dem pulmonalen und vaskulären System führen können. Ein möglicher, funktioneller Mechanismus von RAGE in der pulmonalen Fibrose wurde hier zum ersten Mal beschrieben.

1. Introduction

1.1 The receptor for advanced glycation end products (RAGE)

The receptor for advanced glycation end products (RAGE) is a type I transmembrane receptor of the immunoglobulin superfamily composed of three extracellular immunoglobulin-like domains V, C1, C2, a transmembrane helix and a short, highly negatively charged, cytoplasmatic tail with no known binding motif at the intracellular C-terminus.

Several shorter isoforms exist beside the RAGE full-length receptor. An N-truncated receptor lacking the V-domain and two soluble RAGE isoforms composed of the extracellular domains which can be derived by alternative splicing, called endogenous soluble RAGE (esRAGE) or which arise from cleavage by the matrix metallo-proteases ADAM10 or MMP-9, called soluble RAGE (sRAGE) (Raucci, Cugusi et al. 2008; Zhang, Bukulin et al. 2008). It was shown that calcium is a critical regulator of the intramembrane-proteolysis of RAGE, catalyzed by ADAM10 and the γ-secretase (Galichet, Weibel et al. 2008). The function and possible benefit of the processing of RAGE is broadly unknown and not well understood. However, it is widely accepted that the soluble isoforms of RAGE can intercept and prevent certain ligand interactions with RAGE.

The human gene for RAGE, *ager* (advanced glycation end products receptor), is localized on chromosome 6 in the histocompatibility complex between class II and class III. The *ager* gene is composed of 10 introns and 11 exons which can undergo alternative splicing to derive splice variants. The RAGE-promoter contains nuclear factor (NF)-κB sites, interferon-γ response element and an interleukin-6 (IL-6) DNA binding motif, whereby the NF-κB sites control the expression and connect the expression to inflammation (Bierhaus, Humpert et al. 2005)

1.2 Ligands of the recetor for advanced glycation end products (RAGE)

RAGE was originally identified as a binding receptor for advanced glycation end products (AGE) by Neeper et al. (Neeper, Schmidt et al. 1992).

Nowadays, it is known that RAGE is a multi-ligand receptor, interacting with a wide variety of different molecules such as AGE, β-amyloid peptide, high mobility group binding-protein B1 (HMGB1), S100/Calgranulins and the leukocyte adhesion molecule Mac-1 (CD11b/CD18) (Chavakis, Bierhaus et al. 2003).

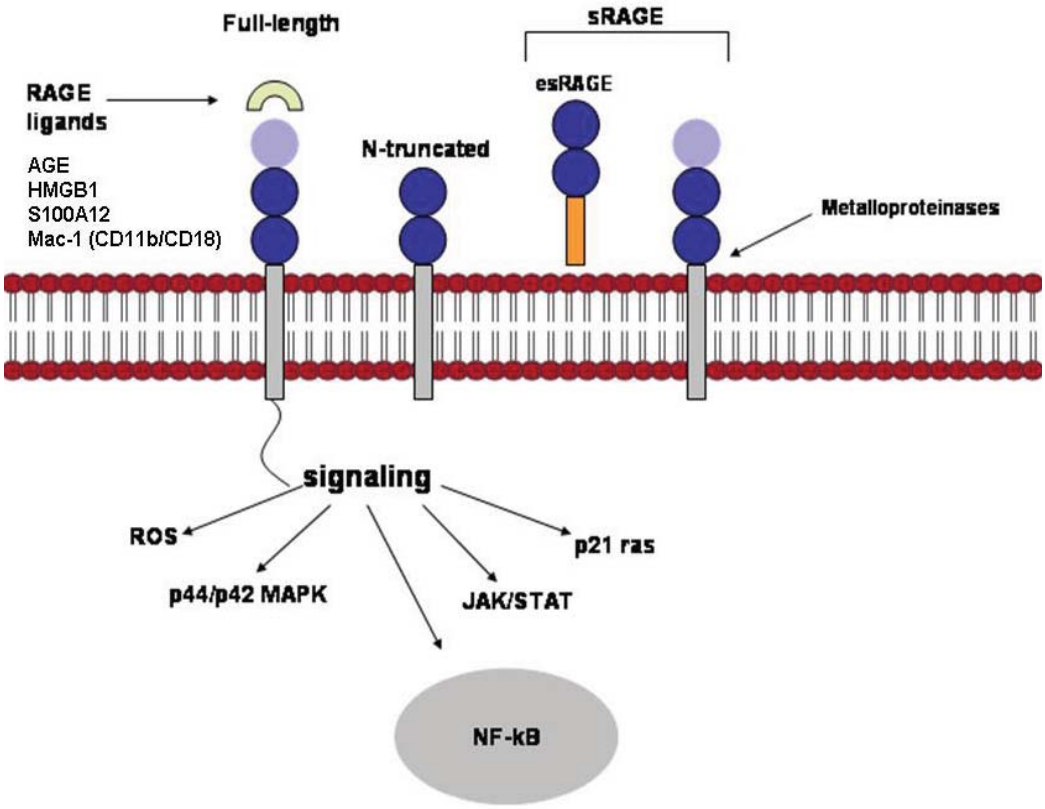

Figure 1: RAGE isoforms and signaling cascade
There are multiple isoforms of the RAGE receptor. The major isoforms are known as full-length RAGE, N-truncated RAGE and soluble RAGE (sRAGE) or endogenous soluble RAGE (esRAGE), The (e)sRAGE receptor is released from the cell and allowed to interact with RAGE ligands prior to their interacting at the plasma membrane. The N-truncated RAGE lacks the intracellular signaling domain, and therefore binds RAGE ligands without directly transducing a signal.

1.2.1 Advanced glycation end products (AGE)

AGE are glycated proteins derived by a non-enzymatic reaction, called Maillard-reaction, between a primary amine (preferably lysine and arginine) and a reducing sugar or an aldehyde, leading to the formation of an initial Schiff-base association product, followed by oxidation, reduction and cross-linking with other amines to Amadori products finally leading to the formation

of carboxymethyllysine (CML), pentosidine or arginine-pyramidine. These AGE are highly heterogenous in their degree of modification and their structural/functional characteristics. Despite this diversity, AGE binds only to the V-domain of RAGE. The binding affinity of AGE to RAGE depends on the degree of glycation of the ligand (10 μM – 100 nM) (Dattilo, Fritz et al. 2007), and the AGE-RAGE interaction can activate p21(ras), MAP Kinase (ERK1/2), MAPK p38 or cdc 42 (Rac) and NF-κB action (Yeh, Sturgis et al. 2001). In addition, AGE can induce NADPH activation and ROS production via RAGE (Yan, Schmidt et al. 1994; Wautier, Chappey et al. 2001).

1.2.2 Amyloid β-peptides

Deposition of amyloid β-peptides (Aβ) occurs during aging and Alzheimer disease in the brain and the cerebral blood vessels. RAGE plays a pro-inflammatory role in neurovascular disorders, by binding soluble amyloid β-peptides and transporting them across the blood-brain barrier via transcystosis (Yan, Chen et al. 1996; Arancio, Zhang et al. 2004; Deane, Wu et al. 2004).

1.2.3 High mobility group box-protein B1 (HMGB1)

The high mobility group box-protein B1 (HMGB1), also known as amphoterin, is a nuclear protein which binds with low affinity to DNA and histones, affecting the chromatin-structure and regulating the binding of steroid hormone receptors, NF-κB and p53 transcription factors (Lotze and Tracey 2005). Despite the intracellular functions, HMGB1 can be released by necrotic cells or secreted by inflammatory cells such as macrophages and monocytes (Rouhiainen, Kuja-Panula et al. 2004; Kokkola, Andersson et al. 2005). Thus, HMGB1 appears to function as an inflammatory mediator and danger signal. Extracellular HMGB1 binds to the V-domain of RAGE with high affinity (~ 7 fold higher than AGE), whereby glycosylation at the V-domain increases the binding affinity of HMGB1 (Srikrishna, Huttunen et al. 2002).

1.2.4 S100/Calgranulins

S100/Calgranulins are calcium binding proteins characterized by two calcium binding elongation factor (EF)-motifs, found in granulocytes, monocytes, macrophages well as induced in epithelial cells under inflammatory conditions. S100/Granulin proteins have a broad spectrum of intracellular functions in cell homeostasis but under cell damage, infection or inflammatory conditions, they convert into cytokine-like mediators which are secreted in a non-classical, Golgi-independent manner, and function as danger signals after release in the extracellular space similar to HMGB1. It was shown that some of S100/Calgranulin proteins such as S100A6 (calcyclin), and S100A12 (EN-RAGE) bind specifically to all three extracellular domains of RAGE (Hofmann, Drury et al. 1999; Xie, Burz et al. 2007).

1.2.5 Mac-1 (CD11b/CD18)

Mac-1 (CD11b/CD18) is a member of the β2-integrin family which is exclusively expressed on the surface of leukocytes. Under inflammatory conditions and in concert with β1-integrins, β2-integrins recognize their counterligands such as ICAM-1, VCAM-1 or surface associated fibrinogen (FBG) on the endothelium, required for integrin-mediated adhesion and diapedesis of activated leukocytes into the inflamed tissue. Recent studies have shown that RAGE mediates leukocyte recruitment *in vivo* based on the RAGE-Mac-1 interaction (Chavakis, Bierhaus et al. 2003) . For the first time, these results shed light on the cell-adhesive functions of RAGE.

The reason for the different binding abilities to interact with such a diversity of ligands may be explained with the concept that RAGE is a pattern recognition receptor (PRP) which recognizes a conserved molecular structure such as the β-sheet fibrilliar structure on diverse ligands. The characteristics of a typical PRP are a multidomain structure, consiting of several similar structural subunits; recognition of diverse types of ligands is brought about by their comman recognition motifs (Gordon 2002). Although RAGE has no similar structural subunits, it clearly fulfills characteristics of a PRP.

1.3 Physiological function of RAGE

RAGE displays high expression during embryogenesis and organ development in the nervous system and the lung (Hori, Brett et al. 1995; Reynolds, Kasteler et al. 2008). After birth, RAGE is downregulated in almost all organs which indicates RAGE's physiological function of RAGE in developmental processes. However, the $RAGE^{-/-}$ mice develops normal with no obvious pathological phenotype (Liliensiek, Weigand et al. 2004). Further studies in neuronal cells showed that activation of RAGE by HMGB1 or S100B can facilitate cell survival by increased expression of the anti-apoptotic protein Bcl-2 (Huttunen, Kuja-Panula et al. 2000). However, the $RAGE^{-/-}$ mice demonstrated neither neuronal deficits nor behavior abnormalities (Wendt, Tanji et al. 2003; Bierhaus, Haslbeck et al. 2004). Further experiments have to be performed to challenge $RAGE^{-/-}$ mice with various stimuli to explore the contribution of RAGE in diverse functions of the organism.

1.4 RAGE expression and its involvement in pathogeneses

The expression pattern of RAGE and its splice-isoforms is tissue- and cell-type specific. Basically, under physiological conditions, the RAGE expression is on a low level and appears to be upregulated under inflammatory conditions via the activation of the NF-κB-promoter or direct ligand-RAGE interaction leads to an amplification of RAGE expression in different cell types (Bierhaus, Humpert et al. 2005).

1.4.1 RAGE in vascular and renal complications of diabetes mellitus

Diabetes mellitus (type I and II) is a multi-phenotypic disease which is characterized by hyperglycemia with subsequent macro- and microvascular late complications, in particular increased atherosclerosis, retinopathy, nephropathy and retinopathy. Under hyperglycemic conditions, the progressive formation of modified proteins, termed advanced glycation end products (AGE), is associated with vascular complications and cellular senescence in diabetic patientens (Brownlee 1995; Hammes, Alt et al. 1999).

Hyperglycemia has direct effects on the vessel wall by promoting glycation and cross-linking of long-living extracellular matrix proteins such as collagen, laminin and vitronectin, involving basement membrane thickening, decrease in proteoglycans density, charge and permeability changes (Hammes, Weiss et al. 1996). Finally, formed AGE induce production of reactive oxygen species (ROS) by activation of NADPH oxidase at least partly through the inflammatory RAGE-signaling in the endothelium as well as in macrophages (Wautier, Chappey et al. 2001; Ding, Kantarci et al. 2007; Gao, Zhang et al. 2008). The AGE-RAGE interaction results in amplification of inflammatory responses by activation of NF-κB (Bierhaus, Schiekofer et al. 2001), production of cytokines such as monocyte chemotactic protein-1 (MCP-1), tumor-necrosis factor-α (TNF-α) (Csiszar and Ungvari 2008), tumor growth factor-β (TGF-β) (Li, Huang et al. 2004) interleukin-1β (IL-1β), tissue factor, endothelin-1 and furthermore to the upregulation of RAGE, the vascular cell adhesion molecules-1 (VCAM-1) and the inter-cellular adhesion molecule-1 (ICAM-1) (Boulanger, Wautier et al. 2002). Under inflammatory conditions, high expression level of endothelial RAGE provides the molecular basis for elevated leukocyte infiltration where leukocyte MAC-1 interacts with its counter-receptor RAGE and facilitates leukocyte recruitment (Chavakis, Bierhaus et al. 2003). In summary, the anti-coagulant endothelium turns into a pro-coagulant cellular surface required for inflammatory signaling.

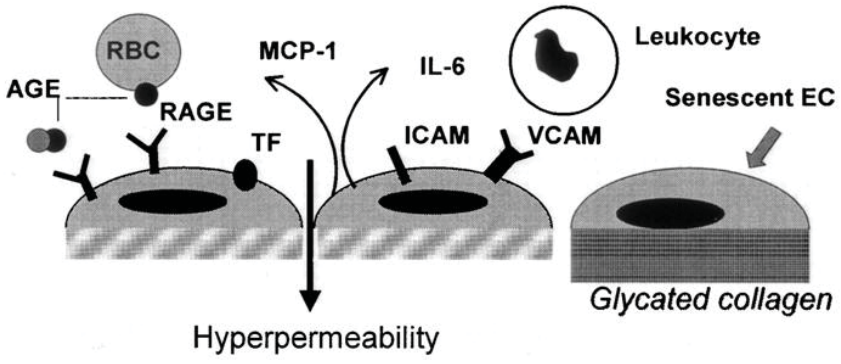

Figure 2: Endothelial dysfunction by AGE-RAGE interaction
AGE-RAGE interaction on endothelial cells induces expression of tissue factor (TF), upregulation of adhesion molecules such as ICAM and VCAM and cytokine release such as MCP-1 and IL-6, followed by leukocyte recruitment and increased permeability of the endothelial monolayer (Wautier and Schmidt 2004).

Diabetic retinopathy and renal fibrosis demonstrates another example where RAGE acts as a pathogenic factor. Despite the fact that AGE and RAGE are co-localized in diabetic kidney (Abel, Ritthaler et al. 1995; Heidland, Sebekova et al. 2001; Hou, Ren et al. 2004), Yamamoto et al. demonstrated in a transgeneic model that diabetic mice over-expressing RAGE developed characteristics of diabetic nephropathy such as kidney enlargement, albuminurea, glomerulosclerosis and tubulointerstitial fibrosis (Yamamoto, Kato et al. 2001). Based on the inflammatory response of RAGE signaling, namely the induction of the main fibrotic cytokine TGF-β as well as inflammatory cell recruitment, several studies indicated a pro-fibrotic role for RAGE due to its involvement in kidney and liver fibrosis (Oldfield, Bach et al. 2001; Forbes, Thallas et al. 2003; Hyogo and Yamagishi 2008).

1.4.2 RAGE in tumor progression and metastasis

Tumor tissue (malignant neoplasm) is characterized by transformed cells which display uncontrolled cell proliferation and impaired cell apoptosis caused by changes on the genetic and epigenetic level. Beside the uncontrolled growth, malignant neoplasm exhibits cellular invasion and often metastasis. Interestingly, HMGB1 is expressed in a wide range of transformed cells indicating a general role of HMGB1 in cell motility and invasive migration of tumor cells. Invasion comprises spatial and temporal coordination. Motility included regulated adhesion to the extracellular matrix and degradation of matrix proteins, resulting in the migration of the cell through the matrix. Receptor-ligand and proteolysis-antiproteolysis reactions regulate the sensing and traction of the moving cell. Here, HMGB1 can function as a generation site for the proteolytic enzyme plasmin. The complex activates pro-matrixmetalloproteases (MMP), resulting in the degradation of extracellular matrix. Forthermore, HMGB1-RAGE interaction leads to proliferation and migration of cells (Taguchi, Blood et al. 2000). The mitogen-activated protein kinase (MAPK) signals p42/p44, p38 and the c-Jun-N-terminal kinase (JNK) are involved in this signal transduction between cell membrane, cytoskeleton and nucleus. The MAPK can be directly activated or indirectly by the GTPases Ras, Rac, Cdc42 and Rho. Activated MAPK

induces gene transcription of adhesion molecules and growth factors as well as modification of myosin and actin filaments of the cytoskeleton. Activation of the master-switch MAPK explains both, the induction of two different cell motions, proliferation and migration.

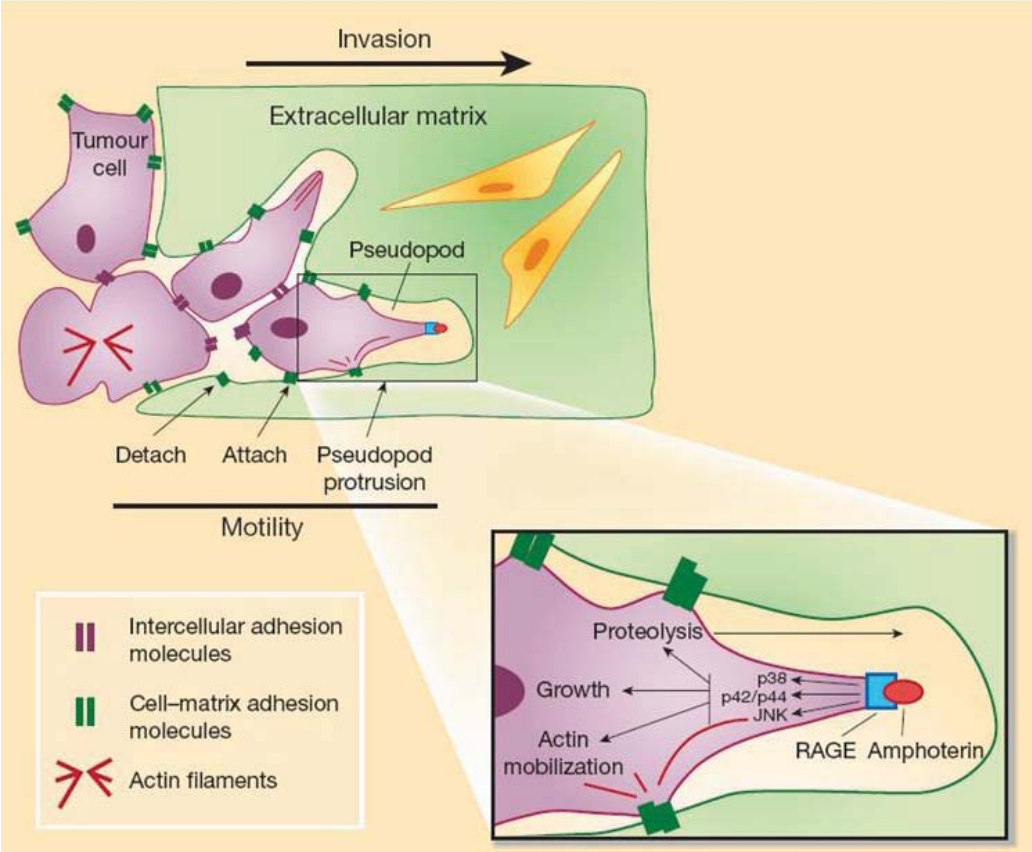

Figure 3: RAGE dependent regulation of cellular invasion.
Invasion can be viewed as cellular motility coupled to regulated adhesion and detachment from the extracellular matrix and proteolysis of extracellular matrix molecules. The advance of pseudopods of the cell — driven by the formation of actin polymers may require the action of cell-surface protein-degrading enzymes, as well as other enzymes, receptors and activators. Extracellular matrix degradation must be balanced by antiproteolysis to allow for adhesive traction. Signal-transduction pathways allow the individual cell to move between phases of pseudopod protrusion, extracellular matrix degradation, antiproteolysis, adhesion and detachment. These pathways split at the level of the mitogen-activating protein kinases JNK, p38 and p42/p44. Blocking the interaction between amphoterin and RAGE suppresses these pathways (Liotta and Clair 2000).

1.4.3 RAGE in innate and adapted immunity

The ability to activate NF-κB and to induce NF-κB regulated adhesion molecules makes RAGE a potent candidate for the regulation of the inflammatory innate immune response upon bacterial infection. Indeed, recent studies showed that RAGE modulates inflammatory responses by

induction of the expression of adhesion molecules such as ICAM-1 and VCAM-1 which enhances the recruitment of inflammatory cells (Fiuza, Bustin et al. 2003; Treutiger, Mullins et al. 2003). Furthermore, RAGE itself functions as a counter-receptor for leukocyte by binding to the β2-integrin Mac-1 and amplifying the leukocyte infiltration. Induced systemic inflammation in the $RAGE^{-/-}$ demonstrated decreased inflammatory cell recruitment (Chavakis, Bierhaus et al. 2003).

In addition, it was shown that RAGE signaling can interact with the toll-like receptor 9 (TLR-9)-pathway, to detect invading pathogens and to distinguished infection-mediated from tissue damage by normal cell necrosis (Tian, Avalos et al. 2007). Under non-infectious cell death, the necrotic cells release HMGB1 which binds to RAGE on plasmacytoid dendritic cells (pDC) or B-cells with no further cell activation. However, under infectious cell death, HMGB1 forms a complex with CpG-containing pathogen DNA, whereby activated RAGE and pathogenic DNA co-interact with TLR9 resulting in interferon-α (IFN-α) secretion or B-cell proliferation. Besides IFN-α production, maturing DC secrete HMGB1 in an autocrine/paracrine manner, leading to RAGE activation and migration of the DC to the drainining lymph nodes, they interact with naive T-cells to establish the T-cell dependent immune-response, indicating that RAGE is involved in DC homing to lymph nodes as well (Dumitriu, Baruah et al. 2005).

1.5 Physiology and pathophysiology of the lung

Oxygen is essential for multicellular aerobic organisms, cellular respiration and ATP synthesis serves as electron acceptor in the respiratory chain. The main function of the lungs is to provide continuous gas exchange between inhaled air and the blood in the pulmonary circulation, supplying oxygen to the organism and removing carbon dioxide, which is then removed from the lungs by expiration. Survival is dependent upon this physiological process being sustained and efficient, whereby this system responses to pathological challenged in different ways to maintain optimal gas exchange.

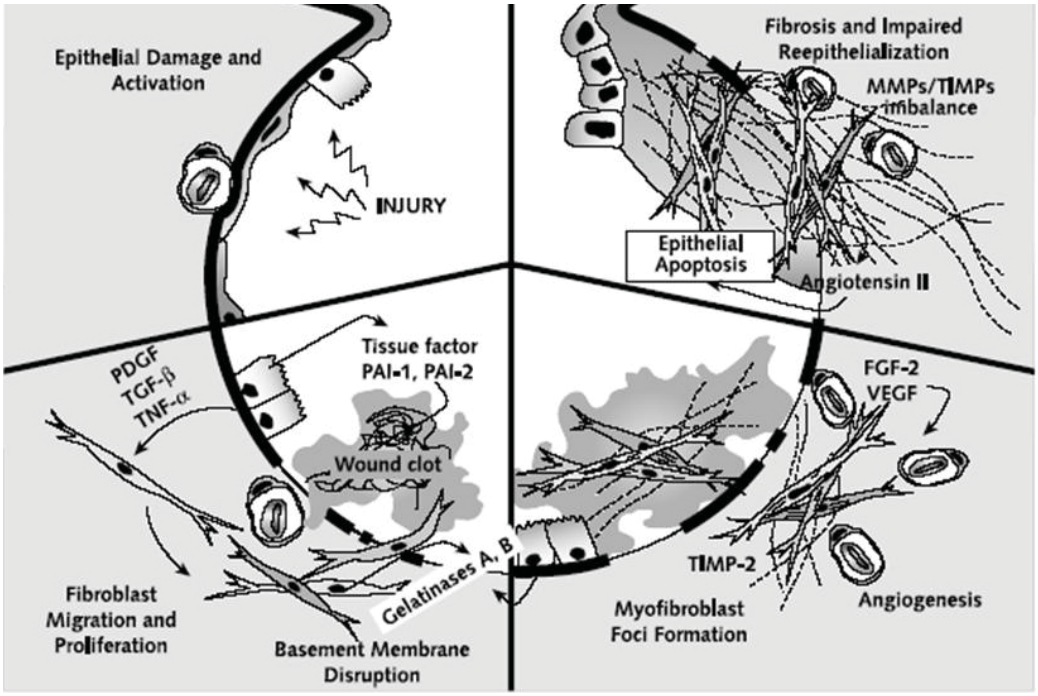

Figure 4: Schematic diagram of lung anatomy
a) Anatomy and localisation of the respiratory tract including Larynx, Trachea and Bronchus. b) cross-section of a bronchus with lining ciliated epithelium and mucin-secreting goblet cells, surrounded by cartilage and smooth muscle cells. c) cross-section of an aloveolar duct at the end of the respiratory bronchiole. The alveolar duct is characterized by an interrupted wall with smooth muscle knobs. d) cross-section of the terminal part of the airway, the alveolus, composed of alveolar epithelia cells capillaries. The outer side is outlined with a surfactant layer (Effros 2006).

1.5.1 Anatomy of the pulmonary system

The respiratory tract extends from the mouth and nose cavities through the bronchial tract down to the distant alveoli. The upper airway serves to filter airborne particles, humidify and warm the inspired gases. The air is passing the larynx, trachea, bronchi, bronchioles (terminal bronchiole) and alveolar duct before reaching the alveolus where the gas exchange takes place between the red blood cells (RBC) in the pulmonary capillaries and the alveolar septae. In the septae three layers (endothelial cells, basallamina and epithelial cells) function as the so called “air-blood barrier” which is very thin (0.1-1.5 µm) and facilitates the diffusion of the gas. The air-blood barrier functions as a barrier which enables the selective exchange between molecules.

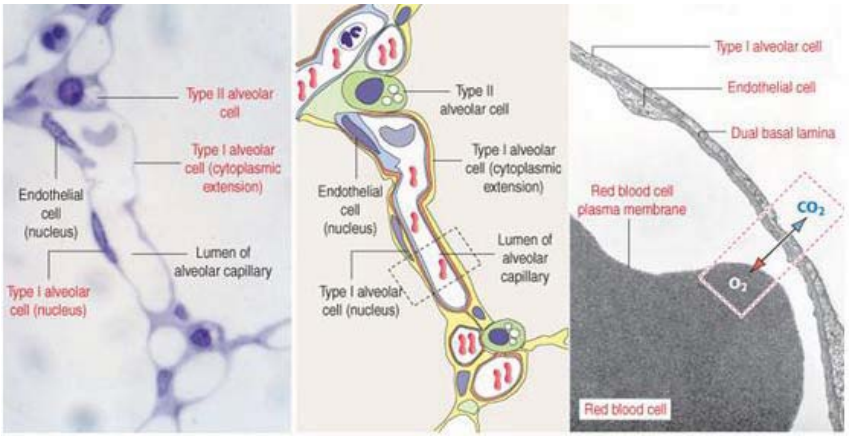

Figure 5: Air-blood barrier
The lung is a gas-exchanging organ for the provision of O_2 to the blood and removel of CO_2 from the blood. Alveolar capillaries are closely apposed to the alveolar lumen. Gas exchange by passive diffusion occurs across the air blood barrier consisting of type I alveolar cells, dual basal lamina, endothelial cells and the plasma membrane of red blood cells. Type II alveolar cells contribute indirectly to the gas-exchange process by secreting surfactant, a lipid-protein complex that reduces the surface tension of the alveolus and prevents alveolar collapsing (Kierszenbaum 2007).

The pulmonary microvascular endothelial cells (PMVEC) form a tight barrier, connected by tight-junctions and desmosomal structures between cells. The endothelial cells are placed on their basolateral side on the basallamina which separates vascular endothelium and pulmonary epithelium. On the alveolar side, the epithelia cells form a tight cellular layer, connected by tight-junctions, facing with their apical side towards the alveolar space. The alveolar epithelium is composed of two different types of alveolar epithelial cells (AEC), whereby the type I cells represent about 40% of the epithelial cells, yet lining 90% of the alveolar surface. Type II cells only cover 10% of the alveolar surface but represent 60% of total cells and are primarily located at the branching of the alveolar septae. Type II cells produce and secrete surfactant (surfactant protein-C positive cells), composed of hydrophobic phospholipid-proteins which maintain alveolar expansion by lowering the surface tension. As putative progenitors, the type II cells are considered to differentiate into type I cells (aquaporin-5 positive cells) (Adamson and Bowden 1974). The interstitium contributes tissue fibroblasts between both layers of alveolar epithelial cells on the alveolar septum, embeded capillaries, and elastic and collagen fibers produced by interstitial fibroblasts.

1.5.2 Interstitial lung diseases

Interstitial lung diseases (ILD), caused by infections or other noxes, is a term for over 200 different lung diseases which are characterized by damage to the lining of the alveoli, increase of the interstitial and/ or vascular spaces, leading to inflammation and fibrosis of the interstitium. A comman symptom in ILD is progressive shortness of breath at rest and more dramatically during physical exercise. The most common ILD include sarcoidosis and usual interstitial pneumonia (UIP).

1.5.3 Idiopathic pulmonary fibrosis

Idiopathic Pulmonary Fibrosis (IPF) is classified as “a specific form of chronic fibrosing interstitial pneumonia of unknown etiology, limited to the lung and associated with the histological entity of usual interstitial pneumonia” (Demedts and Costabel 2002). IPF is a progressive degenerative disease of unknown etiology, for which no effective treatment exists. IPF is characterized histologically by unrestricted interstitial fibroblast proliferation and excessive deposition of extracellular matrix (Maher, Wells et al. 2007).

1.5.4 Pathogenesis of IPF

Although the cause of IPF is still elucidate, it is broadly accepted that the pathogenesis starts with multiple damages to alveolar epithelial cells, resulting in activated epithelial cells which release cellular agonists such as TGF-β, TNF-α, platelet derived growth factor (PDGF), tissue factor (TF) and plasminogen-activator inhibitor 1 (PAI-1) by activated epithelial cells (Selman, King et al. 2001). TGF-β and PDGF induce proliferation and migration of sub-epithelial fibroblasts as well as differentiation to myofibroblasts (Raghu, Masta et al. 1989; Zhang and Phan 1999; Evans, Tian et al. 2003; Khalil, Xu et al. 2005). The primary sites of injury become areas of fibroblast proliferation, forming fibroblast-foci which are sites of active collagen synthesis (Kuhn and McDonald 1991; Tzortzaki, Koutsopoulos et al. 2006). Thus, foci formation is a hallmark of fibrosis. At these sites, epithelial cells and myofibroblasts are producing gelatinases (MMP 9 and 2) which induce

basement membrane disruption to enable the fibroblast/myofibroblast migration to the injured surface. Intra- and interstitial fibroblast/myofibroblast secrete extracellular matrix proteins, mainly collagen. An imbalance between MMP and tissue inhibitors of MMP (TIMP) leads to deposition and accumulation of extracellular matrix proteins (Pardo and Selman 2002). The release of angiogenic factors from fibroblasts such as fibroblast growth factor 2 (FGF-2) and vascular endothelia growth factor (VEGF) leading to angiogenesis to some extent. In parallel, Myofibroblasts show an increased cell survival and delayed apoptosis provoking impaired reepithelialization and tissue fibrosis (Zhang and Phan 1999). The whole sequence of events can be seen as a process of abnormal wound repair where the response to injury is overwhelmed by fibroblasts/myofibroblast proliferation and excessive matrix deposition. Several hypotheses aim to provide the basis for the pathogenesis (Thannickal, Toews et al. 2004; Maher, Wells et al. 2007).

1.5.4.2 Chronic injury hypothesis

Following the original hypothesis, IPF is caused by unknown stimuli which lead to chronic inflammation inducing epithelial injury and subsequent fibrosis. The inflammation theory might represent a major mechanism of ILD such as sarcoidosis or hypersensivity pneumonitis. However, IPF patients display mild or non-inflammatory cell recruitment to fibrotic lesions. In addition, anti-inflammatory drugs such as steroids provide no significant improvement of the pathogenesis (Nadrous, Ryu et al. 2004). These observations lead to the assumption that inflammation is probably not necessary for the development of pulmonary fibrosis (Gross and Hunninghake 2001).

1.5.4.3 Sequential injury hypothesis

The sequential injury hypothesis postulates that IPF is derived from sequential acute lung injury where the repetitive wound repair results in fibrosis by proliferation of fibroblasts, differentiation to myofibroblasts with an contractile phenotype by expression of stress fibers such as α-smooth muscle actin (α-SMA) and the production of collagen. Factors such as

cigarette smoking, viral infection, environmental toxins or genetic background can regulate and modify the fibrotic response (Gross and Hunninghake 2001).

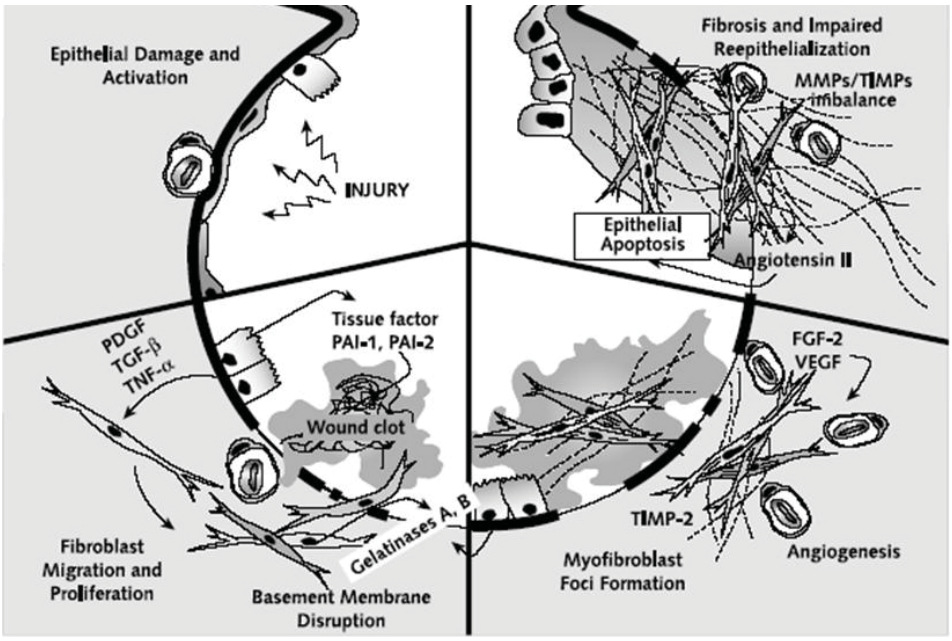

Figure 6: Hypothetical scheme of the abnormal wound healing model for idiopathic pulmonary fibrosis.
Multiple damage and activate alveolar epithelial cells, which in turn induce an antifibrinolytic environment in the alveolar spaces, enhancing wound clot formation. Alveolar epithelial cells secrete growth factors and induce migration and proliferation of fibroblasts and differentiation into myofibroblasts. Subepithelial myofibroblasts may increase basement membrane disruption and allow fibroblast–myofibroblast migration. Interstitial myofibroblasts secrete extracellular matrix proteins, mainly collagens. An imbalance between interstitial collagenases and tissue inhibitors of metalloproteinases provokes the progressive deposit of extracellular matrix and further impairing reepithelialization (Selman, King et al. 2001).

1.5.4.4 Circulating fibrocyte-hypothesis

Philips and colleges discovered a fibroblast-like cell population, sharing leukocyte markers ($CD34^+$ $CD45^+$, $CXCR4^+$, Col I^+ and $Vimentin^+$), called fibrocytes. Fibrocytes are circulating mesenchymal progenitor cells (CMPC) which can differentiate into multiple mesenchymal cell types depending on the tissue environment (Phillips, Burdick et al. 2004). Fibrocytes are believed to be involved in adipogenesis, pulmonary hypertension with associated vascular wall remodeling, wound healing and pulmonary fibrosis. Leukocytes and CMPC are generated in the bone marrow and extravasate to specific region within tissues by trafficking, involving adhesion molecules, chemoattractants and chemoattractant receptors. Lung injury results in high level of the chemokine CXCL12, creating a chemokine gradient for $CXCR4^+$

positive fibrocytes to be released from the bone marrow and recruited from the circulation to the lung (Strieter, Gomperts et al. 2007). In the lung, fibrocytes can proliferate; they differentiate into myofibroblast-like cells with the expression of α-SMA$^+$ and the loss of CD45 and CD34 after the stimulation with TGF-β or endothelin and synthesis to extracellular matrix and thus contribute to pulmonary fibrosis (Gomperts and Strieter 2007; Mehrad, Burdick et al. 2007).

1.5.4.5 Epithelial-mesenchymal transition (EMT) hypothesis

EMT is a well-known process during development where epiblasts undergo a cell phenotype changes early in morphogenesis to form primary mesenchyme. EMT is defined as a process by which differentiated epithelial cells undergo a phenotypic conversion to mesenchymal cells such as fibroblasts and myofibroblasts (Petersen, Nielsen et al. 2003; Radisky, Kenny et al. 2007). The main aspect of EMT is the ability of epithelial cells to lose polarity, disassemble from intracellular arrangements, acquire cell-motility, and move from one location to another. So called secondary EMT which occurs in fully differentiated epithelial cells is an accepted concept in cancer metastasis and kidney fibrosis (Dasari, Gallup et al. 2006; Peinado, Olmeda et al. 2007; Wynn 2008).

The transdifferention of AEC type II to type I cells reflects a normal process of re-epithelialisation after epithelial cell injury where the epithelial cells undergo apoptosis or necrosis. It was proposed that epithelial cells can alternatively undergo transition to a mesenchymal phenotype. This transition is characterized by the loss of epithelial cell markers such as E-cadherin and zonula occludens-1 (ZO-1) and the expression of fibroblast and myofibroblast markers such as fibroblast specific protein (FSP-1), a member of the S100 family, and α-SMA. Thus, cells which are in the process of EMT, express both, epithelial and myofibroblast markers at the same time. Interestingly, the fibrotic cytokine TGF-β has the ability to induce EMT by loss of E-cadherin via Smad-dependent target genes which are mainly controlled by Smad3 (Masszi, Di Ciano et al. 2003). In concert with Smad-independent signaling

such as Rho kinase, Ras, ERK, p38 MAPK, Notch and Wnt proteins, NF-κB or phosphoinositide kinase 3 (PI3K) affect the EMT process as well (Zavadil and Bottinger 2005). The EMT hypothesis provides another explanation for epithelial cell loss and increasing myofibroblast population with excessive extracellular matrix production in pulmonary fibrosis (Willis, duBois et al. 2006).

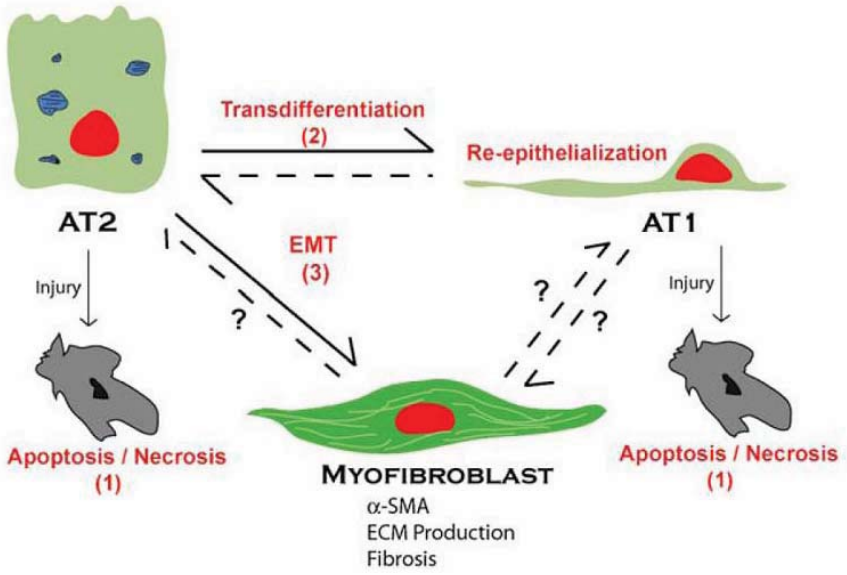

Figure 7: Alveolar epithelial transdifferentiation pathways.
AECs demonstrate pluripotency; under normal conditions, alveolar type II (AT2) cells transdifferentiate into alveolar type I (AT1) cells. Depending on the cellular environment and stimuli, AECs respond to injury by traveling down one of a number of pathways: apoptosis/necrosis (1); proliferation, transdifferentiation, and re-epithelialization (2); or EMT (3) to amyofibroblast phenotype, resulting in extracellular matrix (ECM) deposition, destruction of lung architecture, and fibrosis (Willis, duBois et al. 2006).

1.5.5 Genetic factors

The dominant prevalence of IPF in some families raised the question concerning the genetic background of the disease. Familiar IPF is identified when two or more member of the same family are affected. The precise prevalence is not known but is estimated to be at 7-11 in 100.000 of the population. The familial form of IPF is probably transmitted via an autosomal dominant trait with reduced penetrance (Allam and Limper 2006).

Genetic analysis verified some mutations in the surfactant protein C (SP-C) molecule (Nogee, Dunbar et al. 2001). SP-C is probably the most

hydrophobic protein in the human body, containing a valine, leucine and isoleucine rich domain which forms a stable a-helical structure resulting in insoluble random structures in the aqueous environment. SP-C is secreted by AEC type II cells and facilitates to multify the surface tension in the alveolar space by lining up the alveolar epithelium with a thin lipoproteinlayer. The mutation causes a deletion of 37 amino acids, lacking a cystein residue which is important for protein-disulphide mediated protein folding. In patients with these mutations, the absence of mature SP-C in lung tissue and bronchoalveolar lavage fluid (BAL) was observed, indicating that the precursor protein has not been processed and secreted normally (Nogee, Dunbar et al. 2001).

Recently, in some cases of familiar IPF, germ-line mutations in the genes *htert* and *htr,* encoding telomerase reverse transcriptase and telomerase RNA, was found in familiar cases of IPF (Armanios, Chen et al. 2007). Telomerase reverse transcriptase (hTERT) is a polymerase that conjugates telomere repeats (TTAGGG) to the ends of chromosomes during DNA replication, whereas the telomerase RNA (hTR) provides the template for nucleotide addition. The addition of telomeric repeats to the ends of the chromosome partly re-do the shortening that occurs during DNA replication. Telomeres shorten with each cell division and ultimately activate a DNA damage response that leads to apoptosis. Mutations in *htert* and *htr* affect the telomerase activity and shorten the telomers.

The limited number of familiar IPF patients makes it difficult to perform genetic studies. However, mutations in familiar IPF could be detected in only 1-8% cases, indicating that IPF is a multi-cause disease.

1.6 Animal models of pulmonary fibrosis

Animal models for pulmonary fibrosis are restricted in several ways which has to be considered when results from animal studies are transferred into patient situation (Moore and Hogaboam 2008). Due to the unknown cause of pulmonary fibrosis, several agents are used to induce lung injury with the development of a fibrotic response (Gauldie and Kolb 2008). In addition, the development of symptomatic in patients occurs between 10-20 years of age

(IPF ~ 6 years) whereas the animal model takes only 21-28 days. The most common rodent fibrosis models are here discussed.

1.6.1 Bleomycin model

The bleomycin model is the most commonly used model for lung fibrosis in rodents because of its well characterized feature and the fast development (Adamson and Bowden 1974). Bleomycin is a glycopeptide antibiotic with anti-tumor activity that causes cytotoxic and mutagenic effects by mediating single-strand and double-strand DNA damage in many cell types. Bleomycin can be delivered equelly efficiant to the lung intratracheally, intraperitoneally or intranasally. Bleomycin causes epithelial cell apoptosis and necrosis, followed by an acute inflammation phase (1-7 days) which results in an fibrotic response with increased collagen deposition (day 14) and the establishment of severe fibrotic leasions (day 21-28). However, in this model, fibrosis is self-limiting and starts to resolve after 28 days. Furthermore, this model shows fibrosis untytipical acute inflammatory phase between day one and seven. In addition, the mouse strain Balb/c is rather insensitive towards developing pulmonary fibrosis in this model.

1.6.2 Asbestos, silicia model

Asbestos and silicia such as siliciumoxide can be used to induce pulmonary fibrosis by a persistent fibrotic stimulus which is similary to that observed in humans exposed to occupational dusts and particulates (Bozelka, Sestini et al. 1983). The prolonged presence of the particles in the lung protract cytotoxicity, induce inflammation (to a lower level as compared to the bleomycin-model) and induce the release of cytokines and growth factors. The asbestos model has clinical relevance due to long term exposure in working environment. The clear disadvantage of this fibrosis model takes 12-16 weeks to develop.

1.6.3 Fluorescein isothiocyanate-model

The Fluorescein isothiocyanate (FITC)-model demonstrates a fast fibrotic

response within 14-28 days which varies considerably depending on the amount of FITC (Christensen, Goodman et al. 1999). Although a fast response, the fibrotic response persists at least for six months in Balb/c and C57Bl/6 mice. The big advantage of this approach is the ability to visualize areas of lung injury by the characteristic fluorescence of FITC. However, this model is not of clinical relevance.

1.6.4 Irradiation model

The irradiation model is probably the only model which shows fibrosis development without significant inflammation and therefore the closest model to IPF with clinical relevance (Franko and Sharplin 1994). However, the development of fibrosis takes over 30 weeks and is very cost intensive. Therefore, this model is not commonly used.

1.6.5 Transgenic model

The transgenic model allows studying the effect of a single molecule overexpression in a cell-specific manner. Frequently, the gene of interest is cloned into an adenoviral vector which is used to infect the animal. The adenovirus is transient overexpressing the gene of interest for limited period of time (Bonniaud, Margetts et al. 2003). Recently, the use of transgenetic mice which contain additional DNA or deleted parts of DNA into the genome in every cell, became popular. The gene expression can be controlled by cell-specific promoters, such as SP-C for specific epithelial cell type II expression. However, the amount of expressed protein does not necessarily correspond with physiological levels.

A more accurate way is to control the protein expression by using a transcriptionally-regulated promoter using the tetracycline-resistance operon (Tet-system). Gene expression from this promoter is tightly controlled by the presence or absence of tetracycline or tetracycline derivatives such as doxycycline. In the Tet-On system, the Tet-On activator requires doxycycline for binding the chimeric transcriptional activator. In contrast, in the Tet-Off system doxycycline prevents DNA binding and subsequent gene expression (Gossen and Bujard 1992).

1.7 Hypothesis

Due to its involvement in inflammatory reactions, tissue fibrosis, myoblast and tumor formation, it was hypothesized that RAGE expression in the lung, in contrast to blood vessels, has a protective role in the pulmonary system against degenerative processes, such as IPF pathogenesis.

1.8 Aims

The aim of the study was to investigate the role of RAGE in IPF by addressing the following approches:

First, the expression of RAGE and the cell-specific distribution in lungs from IPF patients and donors was characterized by immunohistology, real-time PCR and western-blot analysis. Furthermore, the expression level of RAGE was investigated in the bleomycin model and compared to the situation in IPF patients.

Second, the regulation of RAGE expression during pulmonary fibrosis development, as well as the effect of pro-fibrotic cytokines on RAGE expression was demonstrated in alveolar epithelial cells and pulmonary fibroblasts.

Third, since cell-proliferation and –migration are key events in pulmonary fibrosis, a potential pathomechanistic role of RAGE was investigated by blocking RAGE with anti-RAGE antibody and siRNA-mediated knock down in epithelial cells and fibroblast and analyzed for cell-proliferation and –migration.

2. Materials

2.1. Chemicals

Acetone	Roth, Karlsruhe, Germany
Acrylamide-Bisacrylamide	Roth, Karlsruhe, Germany
Ammoniumchlorid	Roth, Karlsruhe, Germany
Ammonium persulphate	Roth, Karlsruhe, Germany
Bovine serum albumin Fraction V	Sigma Aldrich
Bromophenol blue	Roth, Karlsruhe, Germany
BCA Protein assay kit	Pierce, Rockford, USA
Bleomycin sulphate	Almirall Prodesfarma, Barcelona, Spain
Calciumchlorid	Roth, Karlsruhe, Germany
Chrystal blue violett	Roth, Karlsruhe, Germany
citrate monohydrate	Roth, Karlsruhe, Germany
(trisodium)-citrate dehydrate	Roth, Karlsruhe, Germany
Collagen I	BD Biosciences, Franklin Lakes, USA
Deoxyribonucleotide triphosphates	Finnzymes, Espoo, Finland
Dimethylsulfoxide	Roth, Karlsruhe, Germany
DL-Dithiothreitol (DTT)	Roth, Karlsruhe, Germany
Dodecyl sodium salt (SDS)	Roth, Karlsruhe, Germany
Dynal magnet	Dynal Biotech, Oslo, Norway
Enhanced Chemiluminescence (ECL) Plus reagents™	GE Healthcare (Amersham), Buckinghamshire, UK
Ethanol	Roth, Karlsruhe, Germany
Eythelene diamino tetra acetic acid (EDTA)	Roth, Karlsruhe, Germany
Formaldehyde alcohol free ≥ 37%	Roth, Karlsruhe, Germany
GenElute mammalian total RNA kit	Sigma Aldrich,St. Louis, USA
Glycerol	Roth, Karlsruhe, Germany
Glycine	Roth, Karlsruhe, Germany
Haematoxylin	Roth, Karlsruhe, Germany
HBSS	Invitrogen (Gibco), Carlsbad, USA
Histostain Plus kit	Zymed Laboratories, San Francisco,

	USA
Hydrochloric acid	Roth, Karlsruhe, Germany
Hydrogen peroxide	Roth, Karlsruhe, Germany
Isofluorane Forene®	Abbott, Wiesbach, Germany
β-mercaptoethanol	Sigma Aldrich,St. Louis, USA
Methanol	Roth, Karlsruhe, Germany
Non-fat dry milk powder	Roth, Karlsruhe, Germany
Mounting medium, Vectashild (with dapi)	Vector Laboratories, Peterborough, UK
Paraffin	Roth, Karlsruhe, Germany
Paraformaldehyde	Roth, Karlsruhe, Germany
Percoll	Sigma Aldrich,St. Louis, USA
Protease Inhibitor cocktail complete™	Roche, Mannheim, Germany
Potassium chloride	Roth, Karlsruhe, Germany
Potassium dihydrogen phosphate	Roth, Karlsruhe, Germany
Rotiphorese® gel 30	Roth, Karlsruhe, Germany
RNasin RNase inhibitor	Promega, Madison, USA
Saline solution, physiological	Baxter, München, Germany
Sodium Chloride	Roth, Karlsruhe, Germany
Sodium dihydrogen phospahate	Roth, Karlsruhe, Germany
Sodium hydrogen carbonate	Roth, Karlsruhe, Germany
SYBR Green PCR master mix	Invitrogen, Carlsbad, USA
N,N,N',N'-Tetramethylethylenediamine (TEMED)	Roth, Karlsruhe, Germany
TransPass R1 transfection Reagent	New England Biolabs, Ipswich, USA
tris(hydroxymethyl)aminomethane (TRIS) base	Roth, Karlsruhe, Germany
Triton-X-100	Roth, Karlsruhe, Germany
Tween 20	Roth, Karlsruhe, Germany
Xylol	Roth, Karlsruhe, Germany

2.1.2 Enzymes

Elastase	Worthington Biochemical Corp, Lakewood, USA
Dispase	BD Biosciences, Franklin Lakes, USA
DNase	Fermentas, Ontario, Canada
ImProm-II reverse transcriptase	Promega, Madison, USA

2.1.3 Cytokines

Hepatocyte growth factor (HGF)	R&D Systems, Minneapolis, USA
Tumor necrosis factor-α(TNF-α)	R&D Systems, Minneapolis, USA
Transforming growth factor-β1 (TGF-β1)	R&D Systems, Minneapolis, USA
Interleukin-1β (IL-1β)	R&D Systems, Minneapolis, USA
keratinocyte growth factor (KGF)	R&D Systems, Minneapolis, USA
High mobility group box (HMGB1)	Sigma Aldrich, St. Louis, USA

2.1.4 Antibodies

anti-RAGE (polyclonal goat)	Biologo, Kronshagen, Germany
anti-RAGE (monoclonal mouse)	Affinity Bio-Reagents, Golden, USA
anti–β1-integrin P4C10 (monoclonal mouse)	Millipore, Billerica, USA
anti–β-actin AC-74 (monoclonal mouse)	Sigma Aldrich, St. Louis, USA
anti-CD14 magnetic beads (monoclonal mouse)	Miltenyi Biotec, Bergisch Gladbach, Germany
anti-vimentin	R&D Systems, Minneapolis, USA
Rhodamine-conjugated anti-goat	Jackson ImmunoResearch, West Grove, USA
HRP-conjugated anti-goat	DakoCytomation, Glostrup, Denmark
HRP-conjugated anti-mouse	DakoCytomation, Glostrup, Denmark
goat control IgG	Millipore, Billerica, USA
mouse control IgG	Sigma Aldrich, St. Louis, USA
human control IgG	Sigma Aldrich, St. Louis, USA

2.1.5 DNA-Primers

Gene	Primer Sequence (5'–3')	
	Forward	Reverse
RAGE (*ager*) (Homo sapiens)	caggaccagggaacctacag	catgtgttgggggctatctt
RAGE (*ager*) (Mus musculus)	gggtgctggttcttgctcta	tggagaaggaagtgcctcaa
hprt-1 (H. sapiens)	aaggaccccacgaagtgttg	gctttgtattttgcttttcca
pbgd (Mus musculus)	atgtccggtaacggcggc	ggtacaaggctttcagcatcgc

2.1.6 Small interfering RNA (siRNA)

Gene	Antisense sequence pool (5'-3')
RAGE (*ager*) (Homo sapiens)	1.ttccattcctgttcattgctt 2.tactgctccaccttctggctt 3.tgttccttcacagatactctt 4.tttgaggagagggctgggctt

2.1.7 General consumable

Eppendorf tubes (0.5 ml, 1.5 ml, 2.0 ml)	Eppendorf, Hamburg, Germany
Falcon tubes (15 ml, 50 ml)	BD Biosciences, Franklin Lakes, USA
Disposable pipettes (2 ml, 5 ml, 10 ml, 25 ml, 50 ml)	BD Biosciences, Franklin Lakes, USA
3MM Whatman paper	GE Healthcare (Amersham), Buckinghamshire, UK
Hybond-C polyvinylidene difluoride (PDVF) membrane	GE Healthcare (Amersham), Buckinghamshire, UK
Pipettes tips (2μl, 20μl, 200 μl, 1000 μl)	Gilson, Middelton, USA

2.1.8 Cell culture

A549 cell line (human)	ATCC, Manassas, USA
Alveolar epithelial cells type II (human)	primary, isolated
Dulbecco's modified Eagle medium (DMEM)	Invitrogen (Gibco), Carlsbad, USA
Fetal bovine serum (FBS)	Invitrogen (Gibco), Carlsbad, USA
Penicillin	Invitrogen (Gibco), Carlsbad, USA
Falcon Petri dishes, cell culture	BD Biosciences, Franklin Lakes, USA
Pulmonary fibroblasts (human)	primary, isolated
Streptomycin	Invitrogen (Gibco), Carlsbad, USA
Trypsin-EDTA	Invitrogen (Gibco), Carlsbad, USA

2.1.9 Machines and systems

Automated microtome RM 2165	Leica Microsystems, Wetzlar, Germany
Dynal magnet	Dynal Biotech, Oslo, Norway
Eppendorf BioPhotometer	Eppendorf, Hamburg, Germany
Eppendorf Centrifuge 5417R	Eppendorf, Hamburg, Germany
Eppendorf Thermomixer comfort	Eppendorf, Hamburg, Germany
Heraeus Instruments Laborfuge 400R	Thermo Scientific, Waltham, USA
Heraeus Centrifuge Mikro20	Thermo Scientific, Waltham, USA
Sequence Detection System 7500	Applied Biosystems
Quantity One software	Bio-Rad Laboratories
Leica DMR fluorescent microscope	Leica Microsystems, Wetzlar, Germany
Methamorph software 7.0	Molecular Devices
CASY Cell Counter System Model DT	Schaerfe Systems

2.2 Patient Population

Lung tissue was obtained from six subjects with IPF and six donor lungs rejected for transplantation (mean age 45.6 ± 15.7 years; 3 females, 3 males). The diagnosis of IPF was made in accordance with American Thoracic Society-European Respiratory Society criteria (2002). All patients exhibited the typical usual interstitial pneumonia (UIP) pattern (mean age 52.4 ± 11.8 years; 2 females, 4 males). The study protocol was approved by the Ethics Committee of the Justus-Liebig-University School of Medicine (AZ 31/93). Informed consent was obtained from each subject for the study protocol.

3 Methods

3.1 Animal Treatment

C57BL/6J mice were purchased from the Jackson Laboratory (Bar Habor, ME) and used for bleomycin challenge to induce pulmonary fibrosis. Bleomycin sulphate (Almirall Prodesfarma, S.A., Barcelona, Spain) was dissolved in sterile saline and applied by microspray as a single dose of 0.08 mg/mouse in a total volume of 200 µl. Control mice received 200 µl of saline. Mice were sacrificed at days 7, 14 and 21 after bleomycin exposure. The lungs were perfused via vasculature and shock frozen or paraffin-immersed for 24 h at room temperature. All experiments were performed in accordance with the guidelines of the Ethics Committee of the University of Giessen, School of Medicine, and approved by local and national authorities.

3.2 Isolation and Culture of Human Alveolar Epithelial Cells type II

Human AEC II cells were isolated, as previously described (Fang X 2006). Cells were isolated after the lungs had been preserved for 4–8 h at 4°C. The pulmonary artery was perfused with a 37°C PBS solution, and the distal air spaces were lavaged with warmed Ca_2- and Mg_2-free PBS solution (0.5 mM EDTA) few times. Afterwards, 13 U/ml elastase in Ca_2-and Mg_2-free HBSS were instilled into the distal air spaces through segmental bronchial intubation.

After digestion for 45 min, the lung was minced finely in the presence of fetal bovine serum (FBS) and DNase (500 μg/ml). The solution was then layered onto a discontinuous Percoll density gradient 1.04 –1.09 g/ml solution and centrifuged at 400 g for 20 min. The upper band containing a mixture of type II cells and alveolar macrophages was collected and centrifuged at 150 g for 10 min. The cell pellet was washed and resuspended in Ca_2- and Mg_2-free PBS containing 5% FBS. The cells were then incubated with magnetic beads coated with anti-CD-14 antibodies at 4°C for 40 min. Then the beads were depleted with a Dynal magnet. The remaining cell suspension was incubated in human IgG-coated tissue culture-treated Petri dishes in a humidified incubator (5% CO_2, 37°C) for 90 min. Unattached cells were collected and counted. The purity of isolated human AEC type II cells was examined by Papanicolaou staining. The purity and viability of AEC preparations was consistently between 90% and 95%.

3.3 Isolation and Culture of Human Pulmonary Fibroblasts

Fibroblasts were isolated from human donor lungs, as described previously (Wang, Zhang et al. 2006). The lungs were perfused via pulmonary artery and lavaged. Lung tissue was dissected from the airways, minced into 2-mm^3 pieces and placed in tissue culture flasks in a humidified incubator at 37°C under 5% CO_2 atmosphere with a minimal volume of DMEM supplemented with 10% FBS, 100 units/ml penicillin, 100 μg/ml streptomycin. An appropriate volume of DMEM medium was then added to the cell culture dishes and the cells were maintained until fibroblasts began to migrate out from the tissue. Identification of fibroblasts was based on the morphology and presence of vimentin staining. Passages 2 to 5 were used for experiments.

3.4 Cytokine Stimulation

Cells were cultured in DMEM containing 0.5% (v/v) FBS for 24 h and 48 h in the absence or presence of TNF-α (10 ng/ml) or TGF-β1 (5 ng/ml) in a humidified incubator at 37°C under 5% CO_2 atmosphere.

3.5 Immunohistochemistry

IPF and donor lung sections were cut in 3-µm thick paraffin sections and transferred onto glass slides and incubated overnight at 37°C. Lung sections were dewaxed by immersion in xylol (3x 10 min) and dehydrated though a series of graded ethanol (2x 100%, 2x 95%, and 2x 70% v/v) 5 min each, followed by PBS washing. Then, the sections were cooked for 20 min in 10 mM citrate buffer (citrate monohydrate and trisodium citrate dehydrate) for antigen retrieval. Potential endogenous peroxidase activity was blocked with 3% (v/v) H_2O_2 for 20 min. The blocking reagent (donkey serum) was applied for 10 min to prevent nonspecific binding. Sections were incubated with the primary anti-RAGE antibody overnight at 4°C. On the following day, tissue slides were incubated with a biotinylated secondary goat antibody for 10 min, followed by streptavidin-conjugated enzyme for another 10 min, and chromogen substrate incubation for 10 min. All the steps described were intermitted by washing 2x 5 min with PBS. Finally, sections were counterstained with haematoxylin for 5 min and washed under running tap water for 10 min. Sections were mounted by mounting medium and sealed with nail polish. The sections were analyzed under a bright field microscope.

3.6 Immunofluorescence

Cells were washed with PBS, fixed with ice-cold methanol for 5 min at -20°C, blocked with 5% (v/v) FBS in PBS for 2 h at room temperature and stained with goat anti-RAGE antibody over night at 4°C, washed four times with PBS and incubated with a rhodamine-conjugated anti-goat secondary antibody in 2.5% (v/v) FBS in PBS for 1 h at room temperature. After intensive washing with PBS (4x 5 min), Sections were mounted by dapi-containing mounting medium and sealed nail polish. The sections were analyzed under a fluorescence microscope.

3.7 siRNA knock down

Cells were seeded and cultured in starvation medium (FBS free DMEM) for 4 h prior to transfection. Cells were transfected using the transfection reagent

TransPass R1 with scrambled siRNA from Santa Cruz or siRNA SMARTpool with the following antisenses: 5'-ttccattcctgttcattgctt-3'; 5'-tactgctccaccttctggctt-3'; 5'-tgttccttcacagatactctt-3' and 5'-tttgaggagagggctgggctt-3'. Transfection reagent was mixed with DMEM without serum, vortexed and incubated for 5 min at room temperature, and the siRNA were added, gently mixed and incubated at room temperature for 20 min. The siRNA-transfection reagent complex was added to the cells. The cells were transfected with 150 nM siRNA and incubated for 24 or 48 h. Afterwards, the cells were harvested and used for downstream applications.

3.8 Reverse Transcriptase (RT)-PCR

Total RNA was extracted from lung tissue and cells using the GenElute™ mammalian total RNA kit, following the manufacturer's instructions. Briefly, 1x 10^6 cells were resuspend in 500 μl lysisbuffer containing β-Mercaptoethanol, pipetted the lysed cells into a filtration column and centrifuged for 2 min. the eluate was diluted with equal volume of 70% ethanol and mixed thoroughly. The mixture was loaded onto a binding column and centrifuged for 15 sec. The flow-through liquid was discard and the binding column washed with washing solution1 (first column wash), centrifuged and washed with washing solution 2 (2x) (second, third column wash). Finally the binding column was transferred to a new collection tube and 20 μl of the elution solution was pipetted onto the binding tube and centrifuged for one additional minute. The RNA concentration of the eluate was determined by measuring the absorbance at 260 nm. All described centrifugation steps were carried out at 14 000 g. 1 μg of total RNA was used for each reverse transcription (RT) reaction. ImProm-II reverse transcriptase, random primers, RNasin ribonuclease inhibitor and dNTPs were used as recommended by manufacture's instructions.

3.9 Real-time PCR

Expression levels of RAGE-mRNA transcripts from human lungs were quantified by real-time PCR. cDNAs were mixed with SYBR Green PCR master mix and primers, and real-time PCR was performed using the

Sequence Detection System 7500. In addition to profiling all samples for the target sequence, samples were profiled for hydroxymethylbilane synthase (hmbs) expression as reference. For each single well amplification reaction, a threshold cycle (CT) was observed in the exponential phase of amplification, and the quantification of relative expression levels was achieved using standard curves for both the target and endogenous controls. Relative transcript abundance of a gene is expressed in ΔCt values ($\Delta Ct = Ct^{reference} - Ct^{target}$).

3.10 Western Blot

Protein extraction from lung tissue samples was performed with minor changes as described before (Xu, Mora et al. 2006). Frozen lung tissue was homogenized under liquid nitrogen with a mortal and suspended in lysis-buffer (50 mM HEPES pH 7.0, 250 mM, NaCl, 5 mM EDTA, 1 mM DTT, and 0.1 % triton-x100). The protein concentration was determined by the BCA Protein Assay Reagent Kit. For western blotting, 20 µg of total lysate was resuspended in Laemmli sample buffer [10% (w/v) SDS, 10 mM β-mercaptoethanol, 20% (v/v) glycerol, 200 mM TRIS-HCl pH 6.8, 0.05% (w/v) bromephenol blue] and resolved on a 10% SDS-PAGE gel for 1.5 h with 80 V and blotted onto a PVDF membrane in a tank blotting system containing transfer buffer [24 mM Tris base, 193 mM glycine, 10% (v/v) methanol] for 1 h and 100 V at 4°C. Afterwards, the membrane was blocked in blocking solution [5% dry-milk (m/v), 1x TBS, 0.01% tween-20 (v/v)] for 2h at room temperature. The membrane was incubated overnight with a primary anti-RAGE antibody in blocking solution at 4°C. Next, the membrane was washed with TBST for 4 x 15 min. A HRP-conjugated secondary antibody was incubated for 1 h in blocking solution at room temperature and washed again 4 x 15 min in TBST afterwards. The membrane was incubated for 5 min with ECL detection reagent to detect the RAGE antibody. Finally, the membrane was stripped with stripping buffer (0.1 M glycine, pH 2.9) washed, blocked and reprobed with an anti-β-actin antibody for loading control.

3.11 Extracellular Matrix Preparation

Adherent fibroblast cells were washed 3x with PBS containing 2% (m/v) BSA and 0.1 mM $CaCl_2$, followed by incubation with 0.5% (v/v) Triton-X-100 in PBS for 15 min at 37°C. Plates were then washed with PBS containing 0.1 M NH_4Cl to remove the cells. Cell-free extracellular matrix (ECM) was blocked with PBS containing 3% (m/v) BSA for 30 min at room temperature.

3.12 Adhesion Assay

Cell adhesion to ECM, collagen (2 μg/ml) or BSA (as control) was tested, as described previously (Chavakis, Kanse et al. 2000). Multiwell plates were coated with collagen (2 μg/ml) or BSA (as control) dissolved in bicarbonatebuffer, (pH 9.6), respectively, and blocked with 3% (w/v) BSA. 1 $x10^4$ cells were plated onto precoated wells as described above in the absence or presence of an anti-RAGE antibody (5 µg/ml), control IgG, anti-β1-integrin antibody (10 µg/ml) or sRAGE (10 µg/ml). After 30 min of incubation in serum-free DMEM, the wells were washed with PBS and Adherent cells were fixed with methanol/acetone (1:1) and stained with crystal violet blue and quantified by absorbance at 590 nm.

3.13 Proliferation Assay

Cell proliferation was determined by cell counting using the CASY Cell Counter System. Cells were transfected with 150 nM siRNA under starvation conditions for 4 h and cultured for further 48 h prior to assess proliferation. KGF (10 ng/ml) and TGF-β1 (10 ng/ml) were used as positive controls for A549 and fibroblast cell proliferation, respectively.

3.14 Migration (chemotaxis) Assay

The migration of cells was analyzed using a Boyden chamber as previously described. Cells were allowed to migrate towards different chemotactic stimuli, including HGF (10 ng/ml) and TGF-β1 (10 ng/ml) or 5% FBS, and the extent of migration was measured by densitometric image analysis with Quantity One software (Bio-Rad Laboratories) and expressed as optical

density/mm².

3.15 Wound Healing Assay

Wound healing assay was performed as previously described (Katsuhiko Asanuma and Mundel 2006). Briefly, cells were seeded overnight in Lab-Tek chamber wells and transfected 48 h prior to scratch. Each coverslip was then scratched with a sterile 200 µl pipette tip, washed with PBS and placed into fresh medium with 5% FBS. After 24 h, cells were fixed with 4% paraformaldehyde and cell nuclei were stained with DAPI. Pictures were captured by fluorescent microscopy under a ×10 objective on a Leica DMR microscope at 0 and 24 h after scratching, and the number of cells that had migrated into the same-sized square fields (marked in fig. 7) were counted with Methamorph software 7.0 (Molecular Devices).

3.16 Basolateral membrane isolation

The basolateral membrane can be easily isolated from a total membrane fraction using a percoll gradient. The used method is based on Hammond et al. (Hammond, Verroust et al. 1994). First, the cell pellets were homogenized in 0.5 ml homogenization buffer (300 mM Mannitol in12 mM Hepes, pH: 7.4 with a pestle device 2x 1 min. the homogenate was centrifuged in a 1.5 ml tube at 2000 g for 8 min to obtain the nuclear pellet. Afterwards, the pellet was rehomogenized in 0.5 ml of homogenization buffer and centrifuged as indicated above. The supernatants were transferred in a prechilled ultracentrifuge tube (polycarbonate 11 x 34 mm) and centrifuged at 14 0000 g for 20 min to obtain a mitochondrial pellet. The supernatant was recovered to another prechilled ultracentrifuge tube and centrifuged at 48.000 g for 30 min in a TLA 100.2 rotor. Next, the pellet was resuspended in 0.3 ml of homogenization buffer, first with the pipette and second with the homogeneizer for 30 seconds. The volume was adjusted to 1 ml with homogenization buffer and 0.2 ml of percoll (16 % gradient) was added and mixed by pipetting. Finally, the samples were centrifuged at 48.000 g for 30 min in a TLS 55 rotor. The basolateral membrane fraction (blurry phase) was

recovered and the quantity of proteins was measured by BCA assay. All steps were performed on ice or 4°C.

4. Statistics

All data were expressed as mean ± SD ($n \geq 3$) unless otherwise indicated. Experimental conditions were compared by using Student's t-test for single measurments or containing multiple comparisons were analyzed using analysis of variance (ANOVA). Differences were considered significant at $p<0.05$. All ΔCt values obtained from qRT-PCR were analyzed for normal distribution using the Shapiro-Wilk-test. Data were assumed to be normally distributed, when $p > 0.05$.

5. Results

5.1 Differential expression of RAGE in mouse tissue

The expression and distribution of RAGE was analyzed in different mouse organs. RAGE was abundantly expressed in the lung, in comparison to other organs, such as the brain or heart, where substantially lower levels of the protein were detected (Fig. 8). The anti-RAGE antibody detected multiple bands of different molecular mass in the lung, which resulted from post-translational modifications of RAGE (Hanford, Enghild et al. 2004).

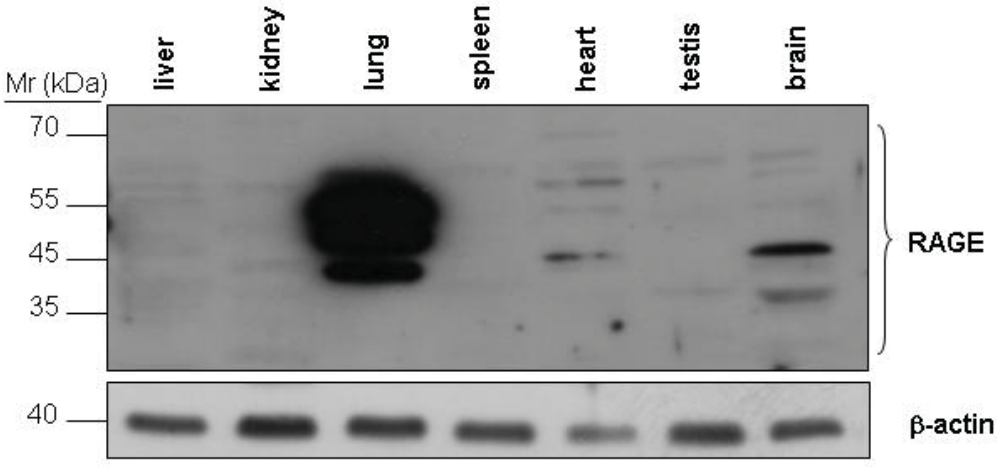

Figure 8: Abundant RAGE expression in the lung.
RAGE expression was appreciably high in the lung and localized to the epithelium. Mouse organ homogenates were prepared and analyzed by western-blot analysis. RAGE exhibited a tissue-specific expression pattern, and was highly expressed in the lung. Three variants were detected (55 kDa, 50 kDa and 45 kDa).

5.2 Distribution of RAGE in donor and IPF lung tissue

In donor lung tissue, RAGE was localized to bronchial epithelial cells, alveolar epithelial cells and pulmonary fibroblasts. In IPF lung sections, RAGE staining was clearly weaker in the bronchial- and alveolar epithelium, as well as in pulmonary fibroblasts (Fig. 9).

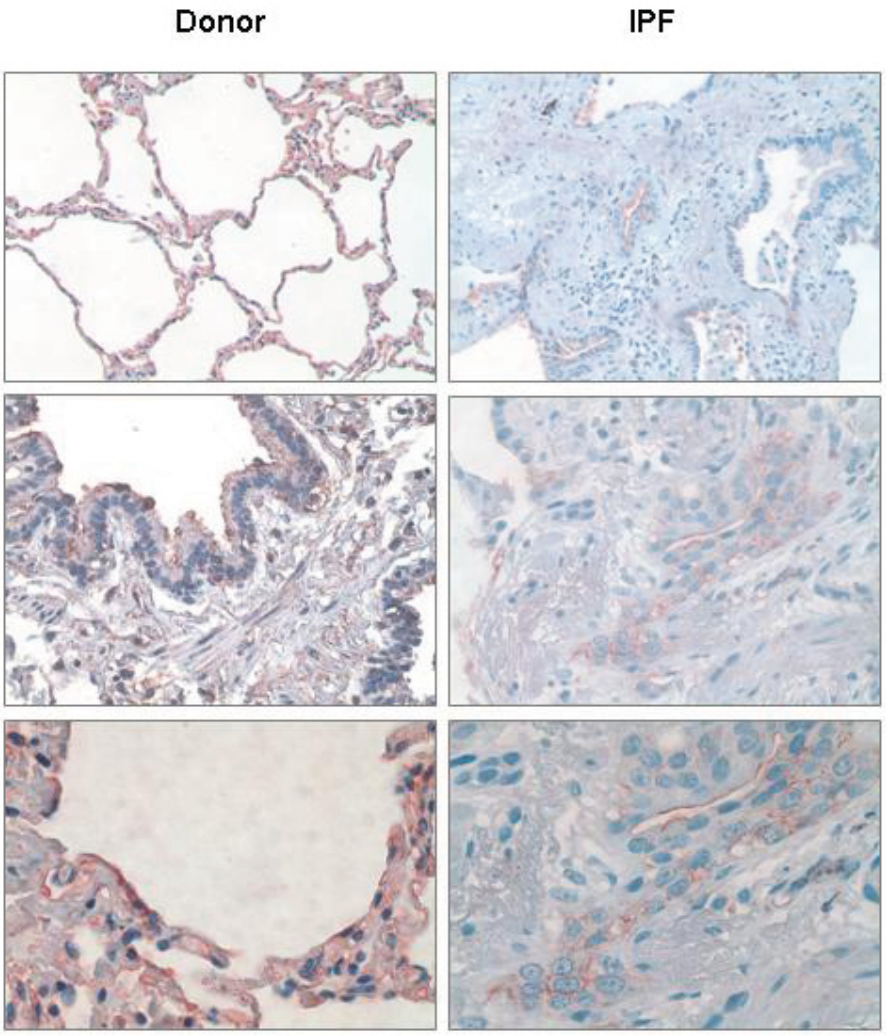

Figure 9: RAGE distribution in IPF and donor lungs.
Human lung sections were stained for RAGE (red) and counterstained with H&E (blue). RAGE was localized to the alveolar and bronchial epithelium as well as to fibroblasts. In comparison to donor lungs, IPF lungs exhibited a weak RAGE staining in alveolar epithelium as well in fibroblasts. Magnification: top panel 20x, middle 40x and bottom 63x.

5.3 RAGE expression in donor, IPF lungs, alveolar type II cells and fibroblasts

RAGE expression at the mRNA and protein level was investigated in IPF (n=6) and donor lung samples (n=6). While the quantitative PCR amplified RAGE transcript in a high amount in all donor samples, it was highly downregulated in the IPF lung homogenates (Fig. 10A). Furthermore, downregulation of RAGE was detected at the protein level in IPF lung

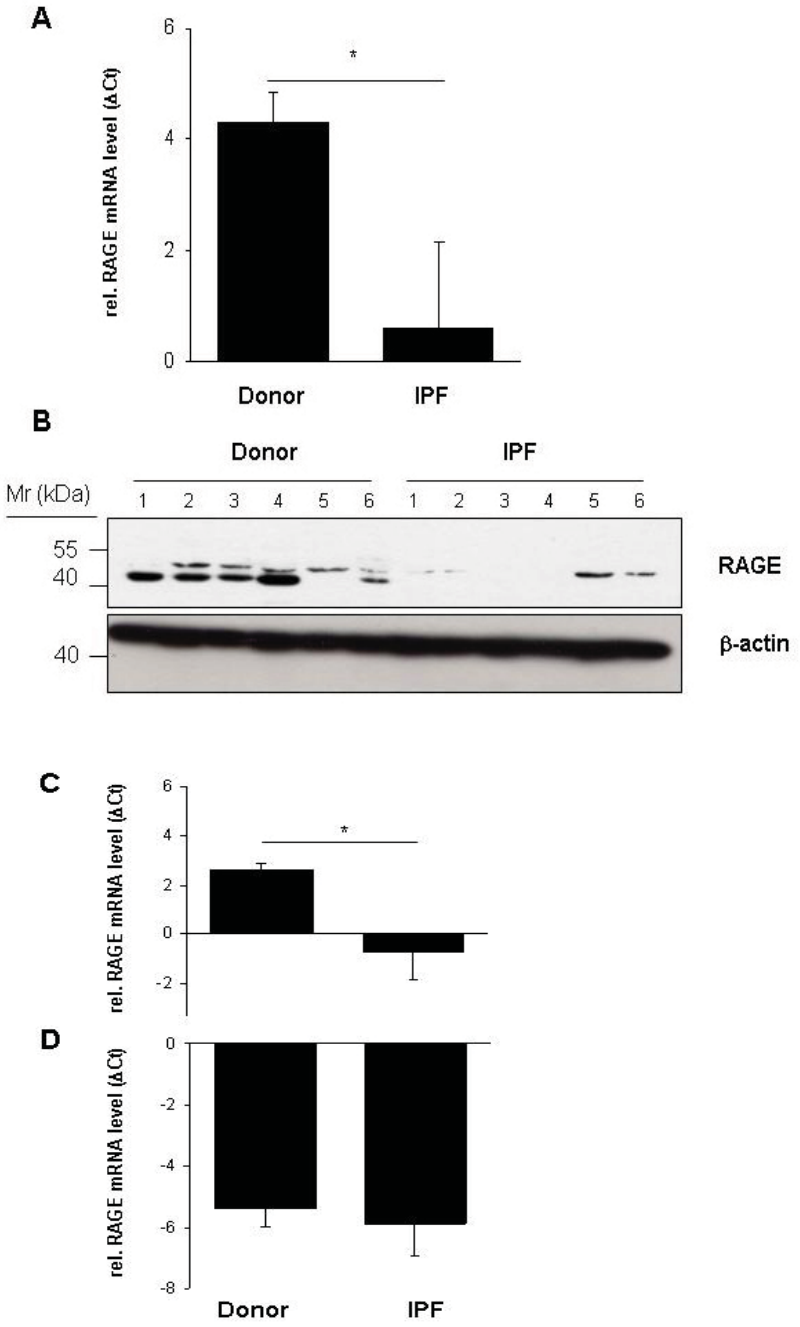

Figure 10: RAGE downregulation in IPF lung homogenate.
(RAGE down-regulation in IPF. (A) RAGE expression was analyzed by real-time PCR in human donor (n 5 6) and IPF (n 5 6) lung homogenates. The RAGE transcript was largely down-regulated in IPF lung homogenates. (B) Proteins from lung homogenates were resolved by SDS-PAGE and analyzed by Western blotting for RAGE detection. RAGE was hardly discernable in all samples from patients with IPF. Two bands of 55 and 45 kD were detected in donor lung homogenates. (C) RAGE expression was evaluated in isolated ATII cells derived from donor and IPF lungs. RAGE mRNA expression was significantly decreased in IPF isolated ATII cells. (D) RAGE expression in isolated pulmonary fibroblasts from donor and IPF lungs did not show any significant differences. Data represent mean 6 SD from at least three separate experiments; *P < 0.01.

homogenates as shown by western blotting. Two major isoforms (55 kDa and 45 kDa) were identified in donor lung homogenates. In contrast, little RAGE was discernable in IPF lung extracts (Fig. 10B). Moreover, there was a significant downregulation of RAGE mRNA levels in IPF derived ATII cells (n=4) as compared to donor ATII cells (n=2) (Fig. 10C). No significant changes were observed between IPF (n=3) and donor (n=3) isolated fibroblasts (Fig. 10D).

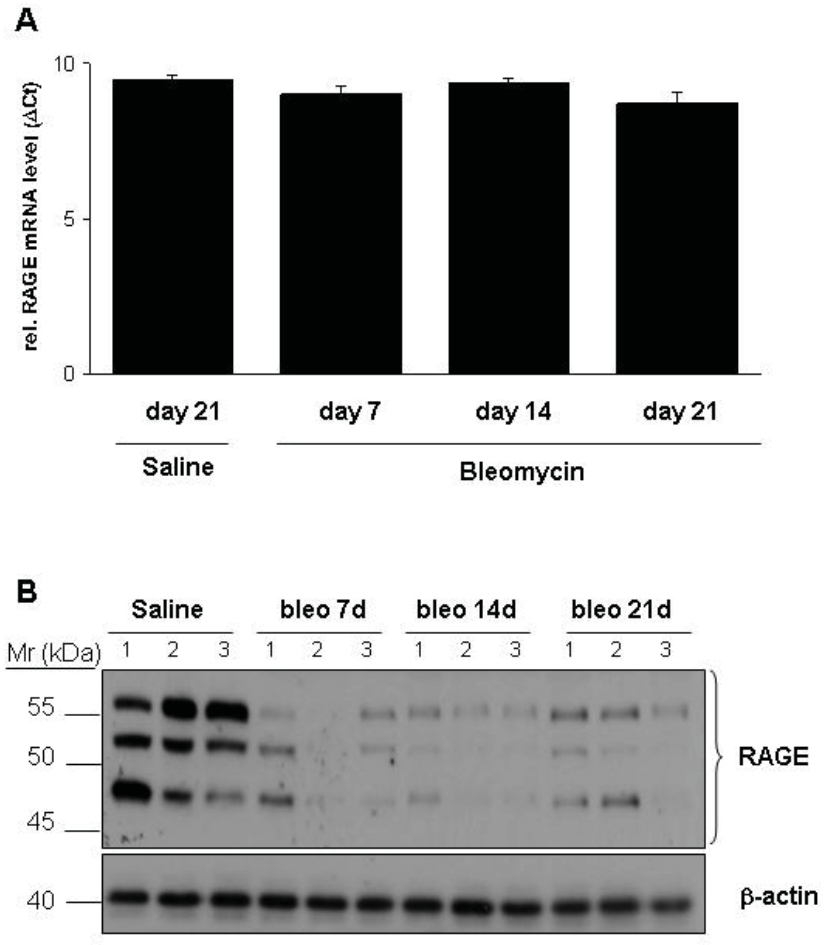

Figure 11 RAGE downregulation in the bleomycin model.
Lung homogenates from saline- and bleomycin-treated mice were analyzed for RAGE expression at the mRNA and protein levels. (A) RNA samples from saline- and bleomycin-treated mice (n 5 3) were subjected to RT-PCR. The RAGE mRNA was amplified in all samples, independent of the time period of bleomycin exposure. No significant changes at the mRNA level were observed after bleomycin treatment. (B) RAGE was significantly down-regulated at the protein level in the bleomycin-treated mice (n 5 3) in comparison with saline-treated mice, as demonstrated by Western blotting.

5.4 RAGE Expression in the bleomycin mouse model of lung fibrosis

To study possible mechanistic relationships between pulmonary fibrosis and the downregulation or loss of RAGE, an established mouse model was employed in which pulmonary fibrosis was provoked by bleomycin inhalation. In bleomycin-treated mice, no significant decrease in RAGE expression was noted at the mRNA level (Fig. 11A). In contrast, at the protein level, RAGE was significantly downregulated in bleomycin treated mice, exemplified by the appearance of very weak protein bands upon western blotting (Fig. 11B). These data are consistent with the observations made on RAGE protein expression in IPF patient lungs. In contrast to the human studies, an additional 50 kDa RAGE variant was detected.

5.5 Influence of Cytokines on RAGE Expression

Since RAGE expression is controlled by cytokines (Tanaka, Yonekura et al. 2000), the influence of TNF-α and TGF-β1 at RAGE mRNA and protein levels was tested in an alveolar epithelial cell line, A549, and primary human pulmonary fibroblasts after 24 and 48 hours stimulation. RAGE expression was significantly altered at the mRNA and protein level by both TNF-α and TGF-β1 in A549 cells after 48 hours as analyzed by quantitative PCR and western blotting (Fig. 12A, B).

In pulmonary fibroblasts, RAGE downregulation at the mRNA level was provoked by TNF-α, and to a lesser extent by TGF-β1 after 24 hour stimulation (Fig. 13A, B). RAGE expression was decreased at the protein level after 48 hours by both cytokines full length RAGE was mainly affected.

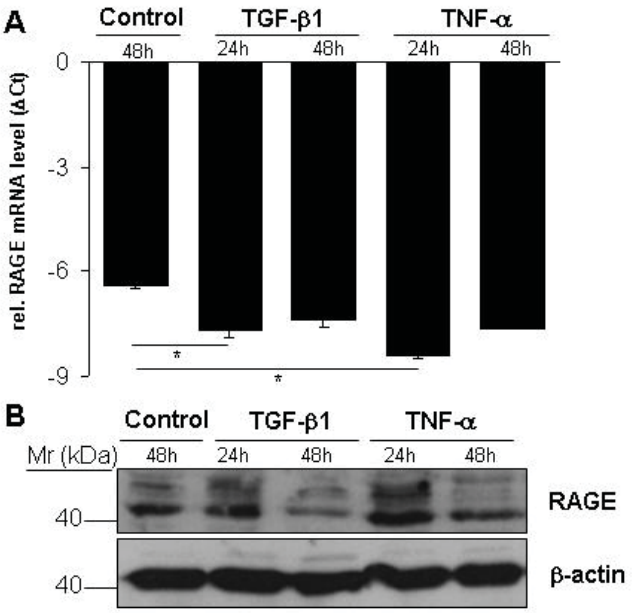

Figure 12: Cytokine-dependent RAGE downregulation in A549 Cells.
The influence of cytokines on RAGE expression was tested in the alveolar epithelial cell line A549 as well as in primary human fibroblasts. RAGE expression was analyzed by immunofluorescence and western-blot analysis after 24 h and 48 h stimulation with different cytokines. Cytokine-treated A549 cells exhibited no changes after treatment with TGF-β1 or TNF-α after 48 h.

5.6 Relation between RAGE and Cell Adhesion, Migration and Proliferation

To further elucidate the mechanism by which a decrease or loss of RAGE would affect cellular functions, cell adhesion, migration and proliferation of A549 cells as well as pulmonary fibroblasts were studied. To examine the role of RAGE-collagen interaction, an adhesion assay with collagen was performed. Blockade of RAGE inhibited cell adhesion on collagen (Fig. 14A) and on intact extracellular matrix (Fig. 14B), suggesting a potential role of RAGE in cell-matrix adhesion. The inhibitory effect of anti-RAGE antibody was diminished by pre-incubation with soluble RAGE (sRAGE).

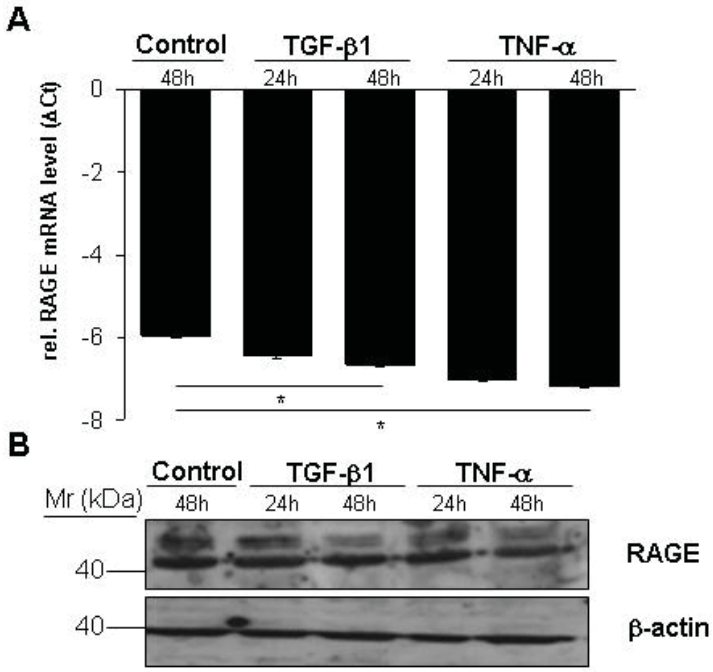

Figure 13:Cytokine-dependent RAGE downregulation in pulmonary fibroblasts.
The influence of cytokines on RAGE expression was tested in primary human fibroblasts. RAGE expression was analyzed by immunofluorescence and western-blot analysis after 24 h and 48 h stimulation with different cytokines. Cytokine-treated fibroblasts were analyzed after 24 h. After stimulation with TNF-α and TGF-β1, the expression of RAGE was decreased. TGF-β1 and TNF-α exposure significantly decreased RAGE expression after 48h. Data represent mean ± SD. from at least three separate experiments. * $p \leq 0.05$.

In contrast, control IgG and sRAGE had no influence on cell adhesion, indicating that the full length RAGE is essential for its adhesive function. In addition, knock down of RAGE by specific siRNA led to increased proliferation of epithelial cells (A549) and fibroblasts as demonstrated by cell counting (Fig. 15 B,C).

Keratinocyte growth factor (KGF) and TGF-β1 served as positive controls for cell proliferation of A549 and pulmonary fibroblasts, respectively. RAGE knock down resulted in increased migration of fibroblasts and epithelial cells (A549) as shown by chemotaxis migration assay (Fig. 15 D). Hepatocyte growth factor (for epithelial cells) and TGF-β1 (for fibroblast) served as positive controls. Undirected chemokinesis was tested by a scratch wound healing assay with siRNA transfected A549 cells and pulmonary fibroblasts. Cells transfected with RAGE specific siRNA migrated faster inducing closure of the scratch, in comparison to scrambled siRNA transfected cells after 24 hours (Fig. 16). siRNA knock down of RAGE in A549 cells affected mainly

cell proliferation, while RAGE knock down in pulmonary fibroblasts resulted in elevated both cell migration and proliferation, but the latter to a lesser extent. RAGE is associated with the cytoskeleton and might regulate proliferation and migration via cytoskeleton re-arrangement (Fig. 17). These data indicate that RAGE is an important component, related to cell adhesion, migration and proliferation of alveolar epithelial cells and pulmonary fibroblasts.

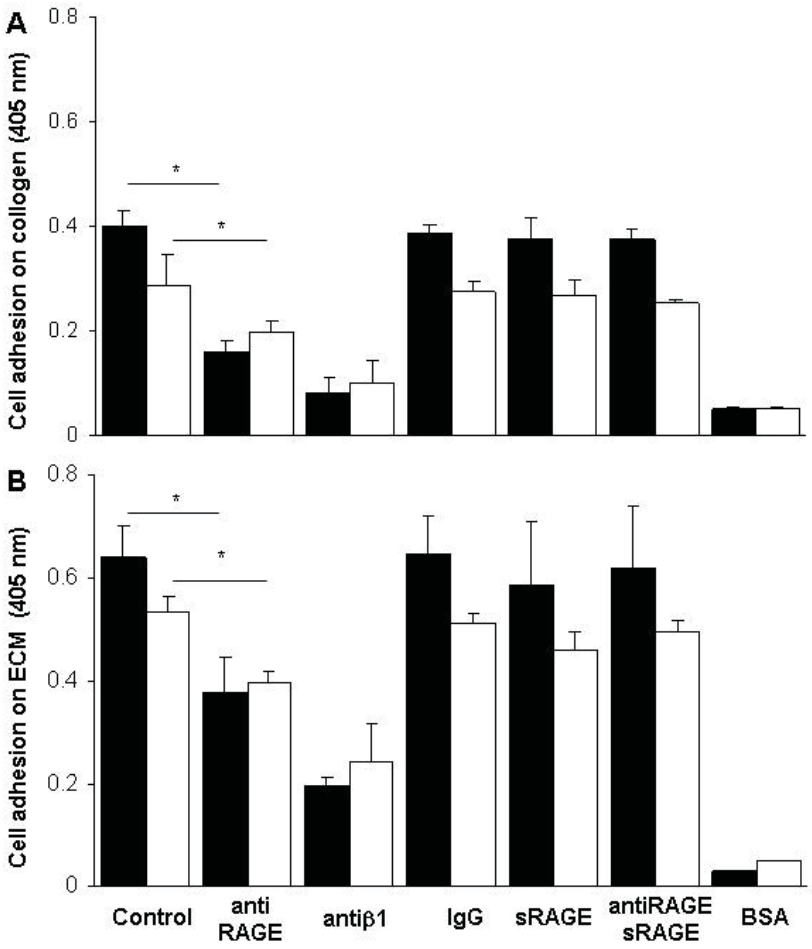

Figure 14: Impairement of cell adhesion on collagen and extracellular matrix by blocking of RAGE.
A549 epithelial cells and primary fibroblasts were incubated with a blocking anti-RAGE antibody and assessed for adhesion to different adhesive substrates. (A, B) The adhesion assay was performed on collagen and extracellular matrix (ECM)-coated plates. Cells treated with the anti-RAGE antibody exhibited significantly decreased adhesion in comparison to control cells. Control IgG and sRAGE had no significant influence on the adhesion. Impaired adhesion was restored by neutralisation of anti-RAGE by sRAGE. As negative control, cells were plated on BSA-coated plates. Data represent mean ± SD. from at least three separate experiments. * $p \leq 0.05$. Filled bars: A549; open bars: fibroblasts.

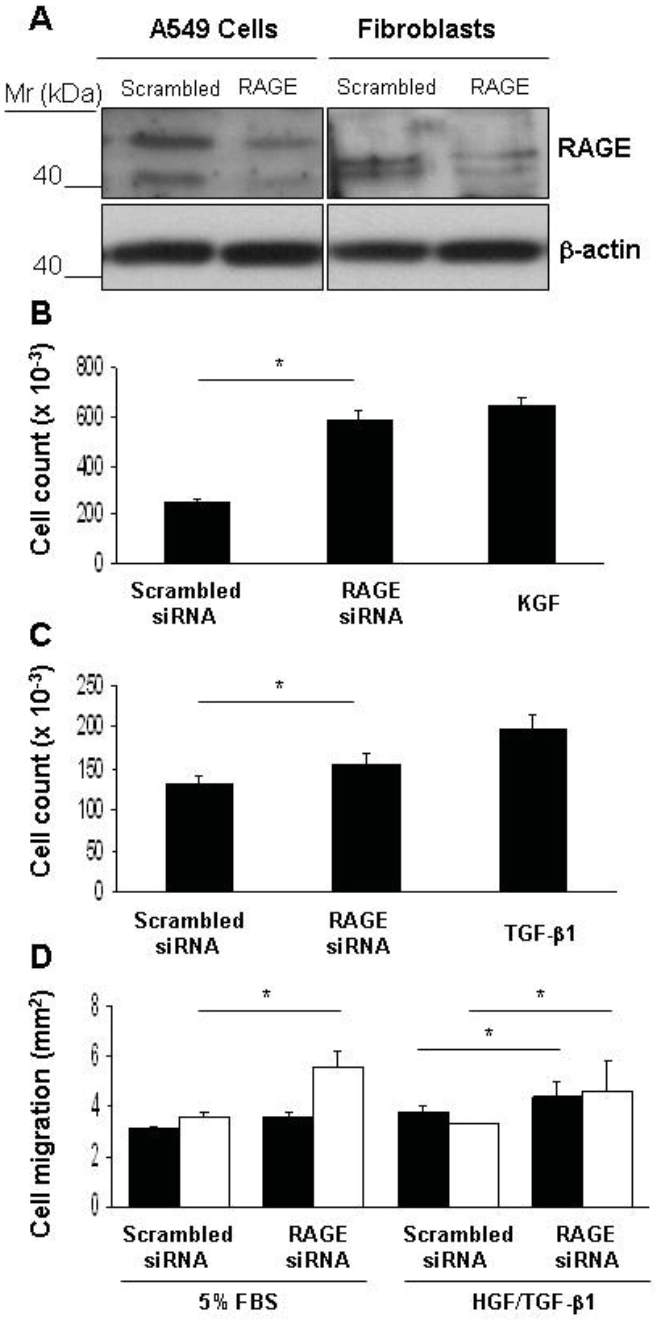

Figure 15: Increased cell proliferation and migration due to siRNA-mediated RAGE knockdown. A549 cells and primary human pulmonary fibroblasts were transfected with specific RAGE siRNA and assessed for cell proliferation and migration. (A) Western blot analysis demonstrated RAGE siRNA knockdown on the protein level in A549 cells and pulmonary fibroblasts. (B) A549 cells transfected with RAGE siRNA exhibited an increased proliferation rate in comparison with scrambled control siRNA. KGF was used as a positive control. (C) Pulmonary fibroblasts transfected with RAGE siRNA exhibited an increased proliferation rate in comparison with scrambled control siRNA. TGF-b1 was used as a positive control. (D) Transfected A549 cells and pulmonary fibroblasts were assessed for chemotactic migration. In more detail, RAGE knockdown with specific siRNA induced a migratory effect as compared with scrambled siRNA in both A549 cells and pulmonary fibroblasts. Data represent means 6 SD from at least three separate experiments; *P < 0.05; filled bars, A549; open bars, fibroblasts.

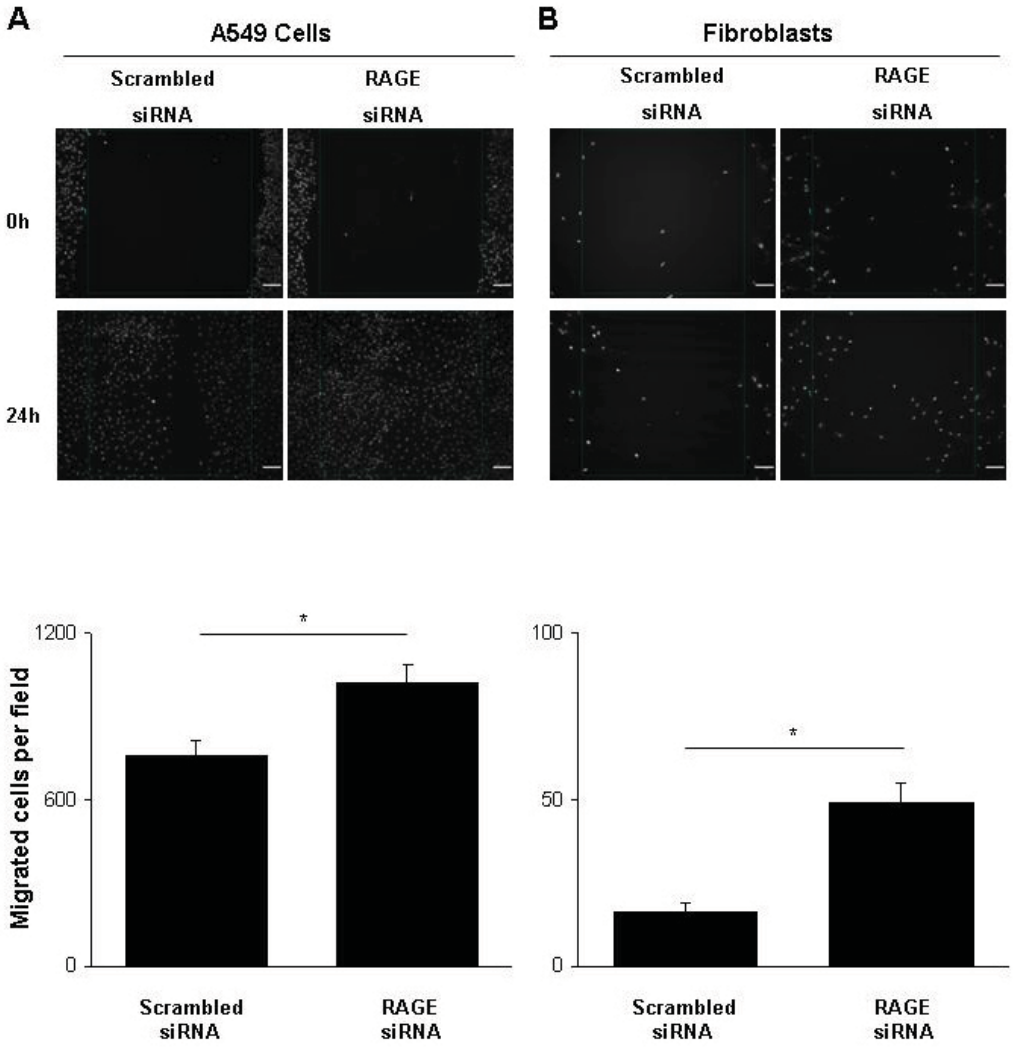

Figure 16: Increased cell migration due to siRNA-mediated RAGE knock down.
A549 cells and primary human pulmonary fibroblasts were transfected with specific RAGE siRNA and assessed for cell migration. (A) A549 cells transfected with RAGE siRNA exhibited an increased migration rate, in comparison to scrambled control siRNA in a Boyden chamber. (B,C) RAGE knockdown induced wound closure. A549 cells and primary human pulmonary fibroblasts were transfected with RAGE-specific siRNA and assessed for wound healing assay. (B) A549 cells transfected with RAGE siRNA exhibited increased migration and wound closure in comparison with scrambled siRNA-transfected cells. (C) Pulmonary fibroblasts exhibited increased migration and wound closure in comparison with scrambled siRNA-transfected cells. Data represent means 6 SD from at least three separate experiments. Scale bar 5 100 mm; *P < 0.05.

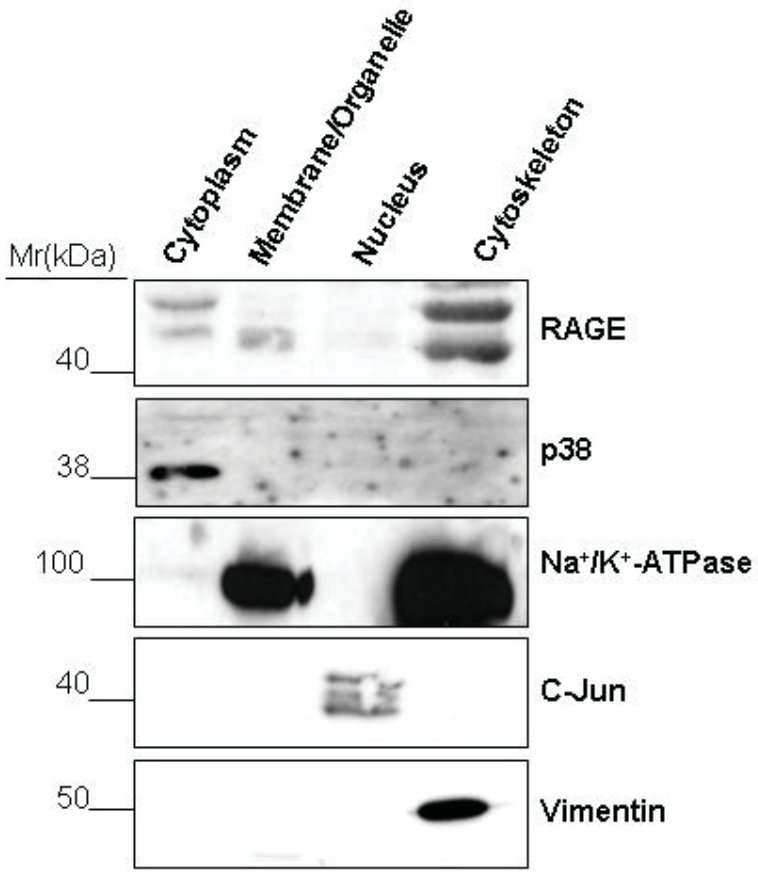

Figure 17: RAGE is associated with the cytoskeleton.
A549 cells were separated by subcellular fractionation and analyzed by western-blot analysis. RAGE was detected in the cytoplasm, the membrane/organelle and predominantly in the cytoskeleton fraction.

6. Discussion

The physiological and pathophysiological role of RAGE in the pulmonary system remains elusive. The following section will reflect the results of the current thesis and will discuss them in the context with the existing literature.

6.1 The role of RAGE in pulmonary fibrosis

In the present work, the relation between RAGE downregulation in fibrotic lungs and the loss of control of cell adhesion, migration and proliferation, alterations believed to be involved in fibrosis development, was described. These data provide new mechanistic insight into the regulatory role of RAGE in cell communication in the lung and are supported by recent findings of other investigators (Hanford LE 2003; Englert, Hanford et al. 2008). Decreased RAGE expression in lungs of IPF patients and in aveolar type II cells (AT II) *in vitro* are in accordance with the observed alterations in the animal model of bleomycin-induced lung fibrosis (Hanford LE 2003).

As demonstrated in this study, downregulation and/or loss of RAGE expression by TNF-α and TGF-β1 in primary human pulmonary fibroblasts and A549 cells as well as its involvement in cell adhesion appear to be processes linked to the onset and/or progression of fibrosis pathogenesis. Here, the profibrotic cytokine TNF-α plays a critical role, possibly driving the inflammatory phase into fibrosis (Miyazaki, Araki et al. 1995; Oikonomou N 2006). Another hallmark of the pathogenesis of pulmonary fibrosis are the alterations in cellular phenotype and functions, accompanied by changes in cell adhesion and communication of lung epithelial cells. The results demonstrate RAGE protein localization mainly on AT I cells, but also on AT II cells, which contain high amounts of RAGE mRNA. It remains to be further established whether RAGE is a specific marker for AT I or AT II epithelial cells (Katsuoka F 1997; Fehrenbach H 1998). Whether these differences are related in any way to the transition from AT II to AT I cells remains to be elucidated. However, it was recently shown the RAGE is upregulated during the transition from AT I to AT II cells (Wang, Edeen et al. 2007). Based on the

these findings, the following function is proposed for RAGE in alveolar epithelial cells.

Under normal physiological conditions AT II cells contain low level of RAGE protein, although there is appreciable RAGE mRNA detactable, allowing the cells to proliferate, and to reepithelialzate. However, during transdifferentiation of AT II cells to AT I cellls, there is increase on RAGE protein levels (Dobbs ref.), which by utelizing with collagen in the ECM, immobilieses AT I cells and thus contributing to there non-proliferative phenotype. RAGE knock down in AT II-like A549 cells as well as pulmonary fibroblasts resulted in elevated proliferative responsiveness to serum and increased cellular motility. Interestingly, RAGE knock down had a more proliferative effect on A549 cells and a higher migratory effect on pulmonary fibroblasts, indicative for a cell type-specific role of RAGE as well. Moreover, the cell phenotype changes provoked by RAGE downregulation in lung fibroblasts are reminiscent of morphological alterations of these cells in IPF, demonstrating increased proliferation and migration in comparison to fibroblasts derived from donors (Suganuma, Sato et al. 1995; Ramos, Montano et al. 2001; Moodley, Scaffidi et al. 2003). Together, RAGE downregulation appears to be associated with both, cytokine and adhesion-related cellular changes and may thus be mechanistically linked to the switch of chronic inflammation to fibrosis in fibrotic lung disease.

The adhesive properties of RAGE in mediating cell-matrix contacts described here and in previous reports (Fehrenbach H 1998; Demling N 2006) appear to be similar and comparable to integrin-mediated adhesion of lung epithelial cells, and loss of RAGE is associated with disturbed cellular contacts. Moreover, preliminary data from our laboratory indicate a tight linkage of RAGE to cytoskeletal elements in lung epithelial cells, suggesting that RAGE provides a regulatory adhesion function linked to cytoskeleton-related signaling systems, also characteristic for integrin functions. It may thus be hypothesized that signaling pathways that would lead to inside-out signaling to affect RAGE function may not be unlikely. Since RAGE was described by our group as the major inflammation-related counter-receptor on endothelial cells for recognition of ß2-integrins on leukocytes (Chavakis, Bierhaus et al.

2003), it remains to be investigated whether loss of RAGE in the aleolar epithelium may lead to disturbances in inflammatory cell interactions in the lung as well. Although the clarification of the cell-stabilizing role of RAGE in the lung requires further work, RAGE appears to serve an "opposite" role in the vasculature, where it becomes upregulated upon inflammatory processes and promotes e.g. leukocyte recruitment into diseased tissue (Chavakis, Bierhaus et al. 2003).

Although the bleomycin model of lung fibrosis used in this study may not necessarily reflect all alterations of fibrosis pathogenesis as observed in humans, data from this *in vivo* model are in accordance with our *in vitro* and *ex vivo* data: A major loss of RAGE expression was seen in these mice that is supported by recent findings from Englert et al. (Englert, Hanford et al. 2008) who indicated that RAGE-/- mice developed more severe asbestos-induced lung fibrosis than wild-type controls, and underlined our data using a different animal model for lung fibrosis. In contrast, He et al. (He, Kubo et al. 2007) reported that RAGE-/- mice were protected from bleomycin-induced lung fibrosis. Furthermore, it has been shown that RAGE levels are decreased in the alveolar epithelium after *in vitro* treatment of rat lung sections with $CdCl_2$ and TGF-β1 (Kasper, Seidel et al. 2004).

Our observations agree with and further complement the findings that RAGE is downregulated in non-small cell lung carcinoma, and its expression impairs the proliferative stimulus of lung fibroblasts on lung cancer cells (Bartling, Hofmann et al. 2005; Bartling, Demling et al. 2006). Thus, loss of RAGE leads to increased cellular proliferation and migration of pulmonary cells in association with different pathologies, and (therapeutic) prevention of RAGE downregulation may serve as a potential antagonizing mechanism in the diseased lung

6.2 RAGE as a biomarker for lung injury

The finding of biomarkers for certain lung diseases is essential for a diagnostic tool and therapy development. Due to its high expression in lung homogenate as well as the appearance of its soluble form in bronchial alveolar fluid (BAL), RAGE was studied as a marker for acute lung injury

(ALI). ALI is often seen as part of a systemic inflammatory process, such as sepsis, with lung manifestations such as widespread destruction of the capillary endothelium, extravascation of protein rich fluid and interstitial edema. Indeed, in an animal model of acute lung injury (ALI), evaluated levels of sRAGE were associated with the severity of the experimentally induced lung injury (Uchida, Shirasawa et al. 2006). in addition, sRAGE was increased in serum samples from patients with acute respiratory distress syndrome (ARDS), a more severe form of ALI (Calfee, Ware et al. 2008). The underlying mechanism for this phenomenon is not clear. It could be noted that under inflammatory conditions metalloproteases such as MMP-9 and ADAM10 proteolytically dissociate RAGE from the epithelial membrane or that epithelial injury-induced apoptosis or necrosis leads to sRAGE release into the alveolar space. The present results show that RAGE is dramatically downregulated in lung homogenate and in alveolar type II cells from IPF patients as well as in the bleomycin model. Furthermore, sRAGE level in BAL from IPF patients is decreased as well (Bargagli, Penza et al. 2008), indicating that RAGE expression is different in pulmonary fibrosis than in acute lung injury. However, RAGE might not be useful as a biomarker for IPF since downregulation of RAGE was observed as well in lung adenocarcinoma (Hofmann, Hansen et al. 2004) (Stav, Bar et al. 2007).

In respect to cell-type specific markers, RAGE was proposed to be an AT I marker (Fehrenbach, Kasper et al. 1998; Shirasawa, Fujiwara et al. 2004). While it remains to be further established whether RAGE is a specific marker for AT I or AT II epithelial cells (Katsuoka F 1997; Fehrenbach H 1998), the present results demonstrate RAGE protein localization mainly in AT I cells, but also in AT II cells, which contain high amounts of RAGE mRNA. Whether these differences are related in any way to the transition from AT II to AT I cells remains to be elucidated.

6.3 RAGE-ligand signaling in the lung

The role of RAGE and its ligands in maintaining and amplifying inflammation has been investigated in several tissues. RAGE-mediated tissue damage is being involved in chronic inflammatory pathology of multiple organs. In the

lung, several RAGE ligands were indentified under inflammatory conditions. AGE accumulation was demonstrated in lung tissue after smoke exposure, and cigarette smoke extract induced RAGE expression via early growth factor-1 (Egr-1) *in vitro* (Morbini, Villa et al. 2006; Reynolds, Kasteler et al. 2008). However, the situation *in vivo* is by far more complex. AGE in the alveolar space have to face several surfactant proteins with AGE-binding properties such as lysozyme and lactoferrin which both contains AGE-binding domains and might contribute to AGE clearence (Li, Tan et al. 1995). In addition, high sRAGE levels are present in BAL and might prevent AGE-RAGE interaction on the alveolar epithelium.

The situation with the S100 proteins is similar, S100A12 (EN-RAGE) and S100B are expressed under inflammatory conditions and in acute lung injury (Morbini, Villa et al. 2006; Wittkowski, Sturrock et al. 2007). However, whether this association indicates a potential pro-inflammatory signaling pathway remain to be unsolved. The most likely interaction could occur between epithelial cell-expressed RAGE and HMGB1, which has the highest affinity for RAGE. HMGB1 is released from injured and necrotic cells. In addition, the concentration of HMGB1 in sepsis, which is associated with acute lung injury, as well as in bleomycin-induced pulmonary fibrosis (He, Kubo et al. 2007), can reach high levels which are unlikely to be blocked completely by endogenous sRAGE. Indeed, applied HMGB1 leads to cytokine release and inflammatory cell recruitment to the lung (Abraham, Arcaroli et al. 2000). However, since RAGE downregulation is taking place early after bleomycin administration as well the fact the RAGE is downregulated in IPF patients (present results), it is more likely that the observed effects are mediated via TLR2 and TLR4 receptors as described before (Tsung, Klune et al. 2007).

6.4 Potential mechanism of RAGE downregulation

The RAGE promoter which is controlled by three NF-κB binding sites links the RAGE expression to inflammation. Thus, it is recognized that RAGE controls inflammation in several diseases (Bierhaus, Humpert et al. 2005). Surprisingly enough, in IPF patients as well as in the bleomycin mouse model,

with its acute inflammatory phase, RAGE is largely downregulated. This phenomenon might be explained by non-classical signaling events.

6.4.1 RAGE downregulation by micro-RNA

In lung homogenate from IPF patients and AT II cells, the RAGE transcripts were downregulted. One possible explanation is that micro-RNA (miRNA) might interact with RAGE mRNA and could regulate its expression. miRNA gene regulation was recently discovered as an additional regulatory mechanism caused by endogenous, 21-nucleotide-long derived miRNA. Similar to siRNA, miRNA can regulated gene transcription as well as translation by degradation or blocking transcripts of translation (Pillai, Bhattacharyya et al. 2007; Flynt and Lai 2008).

The excat pairing between miRNA and target mRNA trigges degradation through a mechanism similar to RNA interferance. However, mostly miRNAs regulate gene expression by imperfect base pairing to the 3' UTR of the target mRNA, causing translational repression or exonucleolytic degradation of target mRNA. The miRNA is incooperated in a ribonucleoprotein complex (miRNP) which is composed of Argonaute proteins which exhibit nucleolytic activity. The RAGE encoding *ager* mRNA transcripts from mouse and human have several potential binding sites for miRNA, indicating a potential gene regulatory mechanism. the functions of these miRNAs are not yet described and need to be further analyzed. However, miRNA-mediated mechanisms might explain the effect of stable RAGE mRNA expression in mice with absence of RAGE on the protein level.

6.4.2 RAGE downregulation by proteases

RAGE mRNA transcripts are not significantly downregulated regulated in the bleomycin model, indicating that other mechanisms are taking place on the post-transcriptional level. ADAM10 and MMP9 are known proteases which mediate RAGE shedding and production/processing of sRAGE (Raucci, Cugusi et al. 2008; Zhang, Bukulin et al. 2008). However, it was recently reported though that sRAGE is downregulated as well in BAL from IPF patients (Bargagli, Penza et al. 2008).

6.4.3 Downregulation of RAGE in relation to caveolae

Another explanation for RAGE downregulation on the protein level could be due to an indirect mechanism where by membrane proteins which are associated with RAGE would be targeted by TGF-β or TNF-α leading to their downregulation together with RAGE. Indeed, it was reported that RAGE is associated with caveolin-rich membrane fractions (Lisanti, Scherer et al. 1994). Caveolin-1, the main component of caveolae, is a critical regulator of lung fibrosis because Caveolin-1 limits TGF-β -induced production of extracellular matrix and restores alveolar epithelial-repair processes. Caveolin-1 expression was markedly reduced in lung tissue from patients with idiopathic pulmonary fibrosis and that this reduction was predominant in alveolar epithelial cells. In addition, fibroblasts had low levels of caveolin-1 expression in patients with idiopathic pulmonary fibrosis (Wang, Zhang et al. 2006; Le Saux, Teeters et al. 2008). Therefore, further investigations should focus on a possible connection between RAGE with caveolae.

6.4 Involvement of RAGE in epithelial-mesenchymal transition

Beside the involvement of RAGE in cell proliferation, RAGE might be involved as well in cell transdifferentiation, especially under conditions of epithelial to mesenchymal transition (EMT). It was reported that AGE can induce EMT by RAGE activation, inducing TGF-β expression in tubulointerstitial fibrosis (Oldfield, Bach et al. 2001). In the lung, induction of EMT by HMGB1 via RAGE in pulmonary fibrosis was suggested (He, Kubo et al. 2007). However, the early downregulation of RAGE in fibrosis can act, if at all, only for a very limited period of time in the onset of the fibrogenesis. Another way for RAGE involvement in EMT can be associated with the present results, suggesting that beside AT II cells also AT I can undergo EMT. Following TGF-β stimulation this process would lead to RAGE downregulation and enables the transformed AT I cells (myofibroblasts) to proliferate excessively and contributes to fibrosis.

6.5 RAGE as an adhesion molecule

Chavakis et al. showed a cell-adhesive function for RAGE, based on the RAGE-Mac-1 interaction, for the first time (Chavakis, Bierhaus et al. 2003). Furthermore, a role for RAGE was proposed in cytoskeleton reorganization and involvement in $\alpha_v\beta_3$ integrin signaling in osteoclasts (Zhou, Immel et al. 2006). The present results indicate a direct interaction between RAGE and the cytoskeleton. In addition, the results show that RAGE can interact with collagen and extracellular matrix. The binding interaction between RAGE and collagen suggests that RAGE might fullfill mainly adhesion function in the lung. RAGE is localised at the basolateral membrane of type I cells, indicative for interaction with collagen of the extracellular membrane (Fehrenbach, Kasper et al. 1998). Surprisingly enough, RAGE-/- mice shows accumulation of macrophages in the lung as opposed to wild-type mice after injury, indicating that RAGE can influence the circulation and adhesiveness of leukocytes (He, Kubo et al. 2007).

The present results supporting a cell-adhesive function for RAGE and show an its physiological relevance in the pulmonary system.

7. Declaration

Herewith, I declare that I have completed this dissertation single-handedly without the unauthorized help of a second party and only with the assistance acknowledged therein. I have appropriately acknowledged and referenced all text passages that are derived literally from or are based on the content of published or unpublished work of others, and all information that relates to verbal communications. I have abided by the principles of good scientific conduct laid down in the charter of the Justus Liebig University of Giessen in carrying out the investigations described in this dissertation.

Der Lebenslauf wurde aus der elektronischen Version der Arbeit entfernt.

The curriculum vitae was removed from the electronic version of the paper.

9. Acknowledgements

I would like to express my deep gratitude to my supervisor Prof. Dr. Klaus T. Preissner who gave me the opportunity to perform my PhD in his laboratory and selected me for the International Training Research group “Signaling Mechanism in Lung Physiology and Disease (SMLPD)”. During this time, he guided me in new directions and let me start to think “outside” the cell. Most of all, he gave me the freedom to perform research in a *Humboldt’sche* way which I highly appreciated and very much enjoyed.

My sincere gratefulness applies to Prof. Dr. Oliver Eickelberg who introduced me to the pulmonary medicine and put great effort in teaching me how science works. Prof. Dr. Oliver Eickelberg encourages the spirit of science to me and the importance of professional ethics. Especially, I would like to thank him for the annual retreat where I could present my research to invited international experts in the field. These scientific workshops were the ideal platform for an intense international exchange with scientists on an informal basis.

Furthermore, I thank the Molecular Biology and Medicine of the Lung (MBML) graduate program and my mentors Prof. Dr. Oliver Eickelberg, Dr. Rory Morty and Dr. Melanie Königshoff for scientific education as good as it gets.

I would like to sincerely thank Prof. Dr. Werner Seeger who established a creative and recognized community in lung science and who demonstrates that the faith in God and science has not to be contradictory.

I thank Prof. Dr. Michael Brownlee from the Albert Einstein College of Medicine, Yeshiva University, who integrated me in his group and treated me as a coequal scientist from the first day. I admire his scientific integrity and his craft to master life.

I specially thank Prof. Dr. Pingoud for his efforts to enable me, as a biochemist, to achieve the *doctor rerum naturalium* from the Justus-Liebig University.

I thank the Deutsche Forschungsgemeinschaft (DFG) for generous financial support in Giessen and New York.

Acknowledgements

I am deeply indebted to my honorable parents for their enormous support in good and bad times throughout my entire life and to my grandparents for their tremendous support and education in many ways.

Special thanks to Heinz Wummel, my mentor in statistics, for his enduring patience.

I am deeply grateful for the help and support of Fotini Kouri who always believed in me and never let me down.

Finally, I thank all my friends around the world, thanks for having you here and there.

10. References

(2002). "American Thoracic Society/European Respiratory Society International Multidisciplinary Consensus Classification of the Idiopathic Interstitial Pneumonias . This Joint Statement of the American Thoracic Society (ATS), and the European Respiratory Society (ERS) was adopted by the ATS Board of Directors, June 2001 and by The ERS Executive Committee, June 2001." Am. J. Respir. Crit. Care Med. **165**: 277-304.

Abel, M., U. Ritthaler, et al. (1995). "Expression of receptors for advanced glycosylated end-products in renal disease." Nephrol Dial Transplant **10**: 1662-7.

Abraham, E., J. Arcaroli, et al. (2000). "HMG-1 as a mediator of acute lung inflammation." J Immunol **165**: 2950-4.

Adamson, I. Y. and D. H. Bowden (1974). "The pathogenesis of bloemycin-induced pulmonary fibrosis in mice." Am J Pathol **77**: 185-97.

Adamson, I. Y. and D. H. Bowden (1974). "The type 2 cell as progenitor of alveolar epithelial regeneration. A cytodynamic study in mice after exposure to oxygen." Lab Invest **30**: 35-42.

Allam, J. S. and A. H. Limper (2006). "Idiopathic pulmonary fibrosis: is it a familial disease?" Curr Opin Pulm Med **12**: 312-7.

Arancio, O., H. P. Zhang, et al. (2004). "RAGE potentiates Abeta-induced perturbation of neuronal function in transgenic mice." EMBO J **23**: 4096-105.

Armanios, M. Y., J. J. Chen, et al. (2007). "Telomerase mutations in families with idiopathic pulmonary fibrosis." N Engl J Med **356**: 1317-26.

Bargagli, E., F. Penza, et al. (2008). "Controversial role of RAGE in the pathogenesis of idiopathic pulmonary fibrosis." Respir Physiol Neurobiol.

Bartling, B., N. Demling, et al. (2006). "Proliferative Stimulus of Lung Fibroblasts on Lung Cancer Cells Is Impaired by the Receptor for Advanced Glycation End-Products." Am. J. Respir. Cell Mol. Biol. **34**: 83-91.

Bartling, B., H.-S. Hofmann, et al. (2005). "Down-regulation of the receptor for advanced glycation end-products (RAGE) supports non-small cell lung carcinoma." Carcinogenesis **26**: 293-301.

Bierhaus, A., K. M. Haslbeck, et al. (2004). "Loss of pain perception in diabetes is dependent on a receptor of the immunoglobulin superfamily." J Clin Invest **114**: 1741-51.

Bierhaus, A., P. M. Humpert, et al. (2005). "Understanding RAGE, the receptor for advanced glycation end products." J Mol Med **83**: 876-86.

Bierhaus, A., S. Schiekofer, et al. (2001). "Diabetes-associated sustained activation of the transcription factor nuclear factor-kappaB." Diabetes **50**: 2792-808.

Bonniaud, P., P. J. Margetts, et al. (2003). "Adenoviral gene transfer of connective tissue growth factor in the lung induces transient fibrosis." Am J Respir Crit Care Med **168**: 770-8.

Boulanger, E., M. P. Wautier, et al. (2002). "AGEs bind to mesothelial cells via RAGE and stimulate VCAM-1 expression." Kidney Int **61**: 148-56.

Bozelka, B. E., P. Sestini, et al. (1983). "A murine model of asbestosis." Am J Pathol **112**: 326-37.

Brownlee, M. (1995). "Advanced protein glycosylation in diabetes and aging." Annu Rev Med **46**: 223-34.

Calfee, C. S., L. B. Ware, et al. (2008). "Plasma receptor for advanced glycation end products and clinical outcomes in acute lung injury." Thorax **63**: 1083-9.

Chavakis, T., A. Bierhaus, et al. (2003). "The pattern recognition receptor (RAGE) is a counterreceptor for leukocyte integrins: a novel pathway for inflammatory cell recruitment." J Exp Med **198**: 1507-15.

Chavakis, T., S. M. Kanse, et al. (2000). "Different mechanisms define the antiadhesive function of high molecular weight kininogen in integrin- and urokinase receptor-dependent interactions." Blood **96**: 514-522.

Christensen, P. J., R. E. Goodman, et al. (1999). "Induction of lung fibrosis in the mouse by intratracheal instillation of fluorescein isothiocyanate is not T-cell-dependent." Am J Pathol **155**: 1773-9.

Csiszar, A. and Z. Ungvari (2008). "Endothelial dysfunction and vascular inflammation in type 2 diabetes: interaction of AGE/RAGE and TNF-alpha signaling." Am J Physiol Heart Circ Physiol **295**: H475-6.

Dasari, V., M. Gallup, et al. (2006). "Epithelial-mesenchymal transition in lung cancer: is tobacco the "smoking gun"?" Am J Respir Cell Mol Biol **35**: 3-9.

Dattilo, B. M., G. Fritz, et al. (2007). "The extracellular region of the receptor for advanced glycation end products is composed of two independent structural units." Biochemistry **46**: 6957-70.

Deane, R., Z. Wu, et al. (2004). "RAGE (yin) versus LRP (yang) balance regulates alzheimer amyloid beta-peptide clearance through transport across the blood-brain barrier." Stroke **35**: 2628-31.

Demedts, M. and U. Costabel (2002). "ATS/ERS international multidisciplinary consensus classification of the idiopathic interstitial pneumonias." Eur Respir J **19**: 794-6.

Demling N, E. C., Kasper M, Laue M, Knels L, Rieber EP (2006). "Promotion of cell adherence and spreading: a novel function of RAGE, the highly selective differentiation marker of human alveolar epithelial type I cells." Cell Tissue Res **323**: 475-88.

Ding, Y., A. Kantarci, et al. (2007). "Activation of RAGE induces elevated O2-generation by mononuclear phagocytes in diabetes." J Leukoc Biol **81**: 520-7.

Dumitriu, I. E., P. Baruah, et al. (2005). "Requirement of HMGB1 and RAGE for the maturation of human plasmacytoid dendritic cells." Eur J Immunol **35**: 2184-90.

Effros, R. (2006). Anatomy, development, and physiology of the lungs, GI Motility online

Englert, J. M., L. E. Hanford, et al. (2008). "A Role for the Receptor for Advanced Glycation End Products in Idiopathic Pulmonary Fibrosis." Am J Pathol.

Evans, R. A., Y. C. Tian, et al. (2003). "TGF-beta1-mediated fibroblast-myofibroblast terminal differentiation-the role of Smad proteins." Exp

Cell Res **282**: 90-100.

Fang X, S. Y., Hirsch J, Galietta LJ, Pedemonte N, Zemans RL, Dolganov G, Verkman AS, Matthay MA. (2006). "Contribution of CFTR to apical-basolateral fluid transport in cultured human alveolar epithelial type II cells." Am J Physiol Lung Cell Mol Physiol **290**: L242-249.

Fehrenbach, H., M. Kasper, et al. (1998). "Receptor for advanced glycation endproducts (RAGE) exhibits highly differential cellular and subcellular localisation in rat and human lung." Cell Mol Biol (Noisy-le-grand) **44**: 1147-57.

Fehrenbach H, K. M., Tschernig T, Shearman MS, Schuh D, Muller M. (1998). "Receptor for advanced glycation endproducts (RAGE) exhibits highly differential cellular and subcellular localisation in rat and human lung." Cell Mol Biol (Noisy-le-grand). **44**: 1147-57.

Fiuza, C., M. Bustin, et al. (2003). "Inflammation-promoting activity of HMGB1 on human microvascular endothelial cells." Blood **101**: 2652-60.

Flynt, A. S. and E. C. Lai (2008). "Biological principles of microRNA-mediated regulation: shared themes amid diversity." Nat Rev Genet **9**: 831-42.

Forbes, J. M., V. Thallas, et al. (2003). "The breakdown of preexisting advanced glycation end products is associated with reduced renal fibrosis in experimental diabetes." FASEB J **17**: 1762-4.

Franko, A. J. and J. Sharplin (1994). "Development of fibrosis after lung irradiation in relation to inflammation and lung function in a mouse strain prone to fibrosis." Radiat Res **140**: 347-55.

Galichet, A., M. Weibel, et al. (2008). "Calcium-regulated intramembrane proteolysis of the RAGE receptor." Biochem Biophys Res Commun **370**: 1-5.

Gao, X., H. Zhang, et al. (2008). "AGE/RAGE produces endothelial dysfunction in coronary arterioles in type 2 diabetic mice." Am J Physiol Heart Circ Physiol **295**: H491-8.

Gauldie, J. and M. Kolb (2008). "Animal models of pulmonary fibrosis: how far from effective reality?" Am J Physiol Lung Cell Mol Physiol **294**: L151.

Gomperts, B. N. and R. M. Strieter (2007). "Fibrocytes in lung disease." J Leukoc Biol **82**: 449-56.

Gordon, S. (2002). "Pattern recognition receptors: doubling up for the innate immune response." Cell **111**: 927-30.

Gossen, M. and H. Bujard (1992). "Tight control of gene expression in mammalian cells by tetracycline-responsive promoters." Proc Natl Acad Sci U S A **89**: 5547-51.

Gross, T. J. and G. W. Hunninghake (2001). "Idiopathic pulmonary fibrosis." N Engl J Med **345**: 517-25.

Hammes, H. P., A. Alt, et al. (1999). "Differential accumulation of advanced glycation end products in the course of diabetic retinopathy." Diabetologia **42**: 728-36.

Hammes, H. P., A. Weiss, et al. (1996). "Modification of vitronectin by advanced glycation alters functional properties in vitro and in the diabetic retina." Lab Invest **75**: 325-38.

Hammond, T. G., P. J. Verroust, et al. (1994). "Heavy endosomes isolated from the rat renal cortex show attributes of intermicrovillar clefts." Am J

Physiol **267**: F516-27.

Hanford, L. E., J. J. Enghild, et al. (2004). "Purification and Characterization of Mouse Soluble Receptor for Advanced Glycation End Products (sRAGE)." J. Biol. Chem. **279**: 50019-50024.

Hanford LE, F. C., Shaefer LM, Enghild JJ, Valnickova Z, Oury TD. (2003). "Regulation of receptor for advanced glycation end products during bleomycin-induced lung injury." Am J Respir Cell Mol Biol. **29**: S77-81.

He, M., H. Kubo, et al. (2007). "The role of the receptor for advanced glycation end-products in lung fibrosis." Am J Physiol Lung Cell Mol Physiol **293**: L1427-36.

Heidland, A., K. Sebekova, et al. (2001). "Advanced glycation end products and the progressive course of renal disease." Am J Kidney Dis **38**: S100-6.

Hofmann, H. S., G. Hansen, et al. (2004). "Discrimination of human lung neoplasm from normal lung by two target genes." Am J Respir Crit Care Med **170**: 516-9.

Hofmann, M. A., S. Drury, et al. (1999). "RAGE mediates a novel proinflammatory axis: a central cell surface receptor for S100/calgranulin polypeptides." Cell **97**: 889-901.

Hori, O., J. Brett, et al. (1995). "The receptor for advanced glycation end products (RAGE) is a cellular binding site for amphoterin. Mediation of neurite outgrowth and co-expression of rage and amphoterin in the developing nervous system." J Biol Chem **270**: 25752-61.

Hou, F. F., H. Ren, et al. (2004). "Enhanced expression of receptor for advanced glycation end products in chronic kidney disease." J Am Soc Nephrol **15**: 1889-96.

Huttunen, H. J., J. Kuja-Panula, et al. (2000). "Coregulation of neurite outgrowth and cell survival by amphoterin and S100 proteins through receptor for advanced glycation end products (RAGE) activation." J Biol Chem **275**: 40096-105.

Hyogo, H. and S. Yamagishi (2008). "Advanced glycation end products (AGEs) and their involvement in liver disease." Curr Pharm Des **14**: 969-72.

Kasper, M., D. Seidel, et al. (2004). "Early signs of lung fibrosis after in vitro treatment of rat lung slices with CdCl2 and TGF-beta1." Histochem Cell Biol **121**: 131-40.

Katsuhiko Asanuma, E. Y.-A., Christian Faul, Yasuhiko Tomino, Kwanghee Kim and a. P. Mundel (2006). "Synaptopodin orchestrates actin organization and cell motility via regulation of RhoA signalling." Nat Cell Biol. **8**: 485-91.

Katsuoka F, K. Y., Arai T, Imuta H, Fujiwara M, Kanma H, Yamashita K. (1997). "Type II alveolar epithelial cells in lung express receptor for advanced glycation end products (RAGE) gene." Biochem Biophys Res Commun. **238**: 512-6.

Khalil, N., Y. D. Xu, et al. (2005). "Proliferation of pulmonary interstitial fibroblasts is mediated by transforming growth factor-beta1-induced release of extracellular fibroblast growth factor-2 and phosphorylation of p38 MAPK and JNK." J Biol Chem **280**: 43000-9.

Kierszenbaum, A. (2007). Histology and Cell Biology. Philadelphia, Mosby Elsevier.

Kokkola, R., A. Andersson, et al. (2005). "RAGE is the major receptor for the proinflammatory activity of HMGB1 in rodent macrophages." Scand J Immunol **61**: 1-9.

Kuhn, C. and J. A. McDonald (1991). "The roles of the myofibroblast in idiopathic pulmonary fibrosis. Ultrastructural and immunohistochemical features of sites of active extracellular matrix synthesis." Am J Pathol **138**: 1257-65.

Le Saux, O., K. Teeters, et al. (2008). "The role of caveolin-1 in pulmonary matrix remodeling and mechanical properties." Am J Physiol Lung Cell Mol Physiol **295**: L1007-17.

Li, J. H., X. R. Huang, et al. (2004). "Advanced glycation end products activate Smad signaling via TGF-beta-dependent and independent mechanisms: implications for diabetic renal and vascular disease." FASEB J **18**: 176-8.

Li, Y. M., A. X. Tan, et al. (1995). "Antibacterial activity of lysozyme and lactoferrin is inhibited by binding of advanced glycation-modified proteins to a conserved motif." Nat Med **1**: 1057-61.

Liliensiek, B., M. A. Weigand, et al. (2004). "Receptor for advanced glycation end products (RAGE) regulates sepsis but not the adaptive immune response." J Clin Invest **113**: 1641-50.

Liotta, L. A. and T. Clair (2000). "Cancer. Checkpoint for invasion." Nature **405**: 287-8.

Lisanti, M. P., P. E. Scherer, et al. (1994). "Characterization of caveolin-rich membrane domains isolated from an endothelial-rich source: implications for human disease." J Cell Biol **126**: 111-26.

Lotze, M. T. and K. J. Tracey (2005). "High-mobility group box 1 protein (HMGB1): nuclear weapon in the immune arsenal." Nat Rev Immunol **5**: 331-42.

Maher, T. M., A. U. Wells, et al. (2007). "Idiopathic pulmonary fibrosis: multiple causes and multiple mechanisms?" Eur Respir J **30**: 835-9.

Masszi, A., C. Di Ciano, et al. (2003). "Central role for Rho in TGF-beta1-induced alpha-smooth muscle actin expression during epithelial-mesenchymal transition." Am J Physiol Renal Physiol **284**: F911-24.

Mehrad, B., M. D. Burdick, et al. (2007). "Circulating peripheral blood fibrocytes in human fibrotic interstitial lung disease." Biochem Biophys Res Commun **353**: 104-8.

Miyazaki, Y., K. Araki, et al. (1995). "Expression of a tumor necrosis factor-alpha transgene in murine lung causes lymphocytic and fibrosing alveolitis. A mouse model of progressive pulmonary fibrosis." J Clin Invest **96**: 250-9.

Moodley, Y. P., A. K. Scaffidi, et al. (2003). "Fibroblasts isolated from normal lungs and those with idiopathic pulmonary fibrosis differ in interleukin-6/gp130-mediated cell signaling and proliferation." Am J Pathol **163**: 345-54.

Moore, B. B. and C. M. Hogaboam (2008). "Murine models of pulmonary fibrosis." Am J Physiol Lung Cell Mol Physiol **294**: L152-60.

Morbini, P., C. Villa, et al. (2006). "The receptor for advanced glycation end products and its ligands: a new inflammatory pathway in lung disease?" Mod Pathol **19**: 1437-45.

Nadrous, H. F., J. H. Ryu, et al. (2004). "Impact of angiotensin-converting

enzyme inhibitors and statins on survival in idiopathic pulmonary fibrosis." Chest **126**: 438-46.

Neeper, M., A. M. Schmidt, et al. (1992). "Cloning and expression of a cell surface receptor for advanced glycosylation end products of proteins." J Biol Chem **267**: 14998-5004.

Nogee, L. M., A. E. Dunbar, 3rd, et al. (2001). "A mutation in the surfactant protein C gene associated with familial interstitial lung disease." N Engl J Med **344**: 573-9.

Oikonomou N, H. V., Zalevsky J, Valavanis C, Kotanidou A, Szymkowski DE, Kollias G, Aidinis V. (2006). "Soluble TNF mediates the transition from pulmonary inflammation to fibrosis." PLoS ONE **1**(e108).

Oldfield, M. D., L. A. Bach, et al. (2001). "Advanced glycation end products cause epithelial-myofibroblast transdifferentiation via the receptor for advanced glycation end products (RAGE)." J Clin Invest **108**: 1853-63.

Pardo, A. and M. Selman (2002). "Molecular mechanisms of pulmonary fibrosis." Front Biosci **7**: d1743-61.

Peinado, H., D. Olmeda, et al. (2007). "Snail, Zeb and bHLH factors in tumour progression: an alliance against the epithelial phenotype?" Nat Rev Cancer **7**: 415-28.

Petersen, O. W., H. L. Nielsen, et al. (2003). "Epithelial to mesenchymal transition in human breast cancer can provide a nonmalignant stroma." Am J Pathol **162**: 391-402.

Phillips, R. J., M. D. Burdick, et al. (2004). "Circulating fibrocytes traffic to the lungs in response to CXCL12 and mediate fibrosis." J Clin Invest **114**: 438-46.

Pillai, R. S., S. N. Bhattacharyya, et al. (2007). "Repression of protein synthesis by miRNAs: how many mechanisms?" Trends Cell Biol **17**: 118-26.

Radisky, D. C., P. A. Kenny, et al. (2007). "Fibrosis and cancer: do myofibroblasts come also from epithelial cells via EMT?" J Cell Biochem **101**: 830-9.

Raghu, G., S. Masta, et al. (1989). "Collagen synthesis by normal and fibrotic human lung fibroblasts and the effect of transforming growth factor-beta." Am Rev Respir Dis **140**: 95-100.

Ramos, C., M. Montano, et al. (2001). "Fibroblasts from idiopathic pulmonary fibrosis and normal lungs differ in growth rate, apoptosis, and tissue inhibitor of metalloproteinases expression." Am J Respir Cell Mol Biol **24**: 591-8.

Raucci, A., S. Cugusi, et al. (2008). "A soluble form of the receptor for advanced glycation endproducts (RAGE) is produced by proteolytic cleavage of the membrane-bound form by the sheddase a disintegrin and metalloprotease 10 (ADAM10)." FASEB J **22**: 3716-27.

Reynolds, P. R., S. D. Kasteler, et al. (2008). "RAGE: developmental expression and positive feedback regulation by Egr-1 during cigarette smoke exposure in pulmonary epithelial cells." Am J Physiol Lung Cell Mol Physiol **294**: L1094-101.

Rouhiainen, A., J. Kuja-Panula, et al. (2004). "Regulation of monocyte migration by amphoterin (HMGB1)." Blood **104**: 1174-82.

Selman, M., T. E. King, et al. (2001). "Idiopathic pulmonary fibrosis: prevailing and evolving hypotheses about its pathogenesis and

implications for therapy." Ann Intern Med **134**: 136-51.
Shirasawa, M., N. Fujiwara, et al. (2004). "Receptor for advanced glycation end-products is a marker of type I lung alveolar cells." Genes Cells **9**: 165-74.
Srikrishna, G., H. J. Huttunen, et al. (2002). "N -Glycans on the receptor for advanced glycation end products influence amphoterin binding and neurite outgrowth." J Neurochem **80**: 998-1008.
Stav, D., I. Bar, et al. (2007). "Usefulness of CDK5RAP3, CCNB2, and RAGE genes for the diagnosis of lung adenocarcinoma." Int J Biol Markers **22**: 108-13.
Strieter, R. M., B. N. Gomperts, et al. (2007). "The role of CXC chemokines in pulmonary fibrosis." J Clin Invest **117**: 549-56.
Suganuma, H., A. Sato, et al. (1995). "Enhanced migration of fibroblasts derived from lungs with fibrotic lesions." Thorax **50**: 984-9.
Taguchi, A., D. C. Blood, et al. (2000). "Blockade of RAGE-amphoterin signalling suppresses tumour growth and metastases." Nature **405**: 354-60.
Tanaka, N., H. Yonekura, et al. (2000). "The Receptor for Advanced Glycation End Products Is Induced by the Glycation Products Themselves and Tumor Necrosis Factor-alpha through Nuclear Factor-kappa B, and by 17beta -Estradiol through Sp-1 in Human Vascular Endothelial Cells." J. Biol. Chem. **275**: 25781-25790.
Thannickal, V. J., G. B. Toews, et al. (2004). "Mechanisms of pulmonary fibrosis." Annu Rev Med **55**: 395-417.
Tian, J., A. M. Avalos, et al. (2007). "Toll-like receptor 9-dependent activation by DNA-containing immune complexes is mediated by HMGB1 and RAGE." Nat Immunol **8**: 487-96.
Treutiger, C. J., G. E. Mullins, et al. (2003). "High mobility group 1 B-box mediates activation of human endothelium." J Intern Med **254**: 375-85.
Tsung, A., J. R. Klune, et al. (2007). "HMGB1 release induced by liver ischemia involves Toll-like receptor 4 dependent reactive oxygen species production and calcium-mediated signaling." J Exp Med **204**: 2913-23.
Tzortzaki, E. G., A. V. Koutsopoulos, et al. (2006). "Active remodeling in idiopathic interstitial pneumonias: evaluation of collagen types XII and XIV." J Histochem Cytochem **54**: 693-700.
Uchida, T., M. Shirasawa, et al. (2006). "Receptor for advanced glycation end-products is a marker of type I cell injury in acute lung injury." Am J Respir Crit Care Med **173**: 1008-15.
Wang, J., K. Edeen, et al. (2007). "Differentiated human alveolar epithelial cells and reversibility of their phenotype in vitro." Am J Respir Cell Mol Biol **36**: 661-8.
Wang, X. M., Y. Zhang, et al. (2006). "Caveolin-1: a critical regulator of lung fibrosis in idiopathic pulmonary fibrosis." J Exp Med **203**: 2895-906.
Wautier, J. L. and A. M. Schmidt (2004). "Protein glycation: a firm link to endothelial cell dysfunction." Circ Res **95**: 233-8.
Wautier, M. P., O. Chappey, et al. (2001). "Activation of NADPH oxidase by AGE links oxidant stress to altered gene expression via RAGE." Am J Physiol Endocrinol Metab **280**: E685-94.
Wendt, T. M., N. Tanji, et al. (2003). "RAGE drives the development of

glomerulosclerosis and implicates podocyte activation in the pathogenesis of diabetic nephropathy." Am J Pathol **162**: 1123-37.

Willis, B. C., R. M. duBois, et al. (2006). "Epithelial origin of myofibroblasts during fibrosis in the lung." Proc Am Thorac Soc **3**: 377-82.

Wittkowski, H., A. Sturrock, et al. (2007). "Neutrophil-derived S100A12 in acute lung injury and respiratory distress syndrome." Crit Care Med **35**: 1369-75.

Wynn, T. A. (2008). "Cellular and molecular mechanisms of fibrosis." J Pathol **214**: 199-210.

Xie, J., D. S. Burz, et al. (2007). "Hexameric calgranulin C (S100A12) binds to the receptor for advanced glycated end products (RAGE) using symmetric hydrophobic target-binding patches." J Biol Chem **282**: 4218-31.

Xu, J., A. L. Mora, et al. (2006). "Increased bleomycin-induced lung injury in mice deficient in the transcription factor T-bet
10.1152/ajplung.00006.2006." Am J Physiol Lung Cell Mol Physiol **291**: L658-667.

Yamamoto, Y., I. Kato, et al. (2001). "Development and prevention of advanced diabetic nephropathy in RAGE-overexpressing mice." J Clin Invest **108**: 261-8.

Yan, S. D., X. Chen, et al. (1996). "RAGE and amyloid-beta peptide neurotoxicity in Alzheimer's disease." Nature **382**: 685-91.

Yan, S. D., A. M. Schmidt, et al. (1994). "Enhanced cellular oxidant stress by the interaction of advanced glycation end products with their receptors/binding proteins." J Biol Chem **269**: 9889-97.

Yeh, C. H., L. Sturgis, et al. (2001). "Requirement for p38 and p44/p42 mitogen-activated protein kinases in RAGE-mediated nuclear factor-kappaB transcriptional activation and cytokine secretion." Diabetes **50**: 1495-504.

Zavadil, J. and E. P. Bottinger (2005). "TGF-beta and epithelial-to-mesenchymal transitions." Oncogene **24**: 5764-74.

Zhang, H. Y. and S. H. Phan (1999). "Inhibition of myofibroblast apoptosis by transforming growth factor beta(1)." Am J Respir Cell Mol Biol **21**: 658-65.

Zhang, L., M. Bukulin, et al. (2008). "Receptor for advanced glycation end products is subjected to protein ectodomain shedding by metalloproteinases." J Biol Chem.

Zhou, Z., D. Immel, et al. (2006). "Regulation of osteoclast function and bone mass by RAGE." J Exp Med **203**: 1067-80.